Research Square

Preprints are preliminary reports that have not undergone peer review.
They should not be considered conclusive, used to inform clinical practice,
or referenced by the media as validated information.

A single-cell and bulk transcriptome meta-analysis reveals RYR2 as a key biomarker and potential regulator in Type 2 Diabetes

Anandwardhan Hardikar

a.hardikar@westernsydney.edu.au

Western Sydney University https://orcid.org/0000-0001-5587-2090

Hrishikesh Hardikar

Western Sydney University

Wilson Wong

Western Sydney University

Supreethi Kanta

Western Sydney University

Rajveer Shekhawat

Western Sydney University

Alexie Papanicolaou

Western Sydney University

Md. Shahidul Islam

Western Sydney University

Rashmi Prasad

Lund University https://orcid.org/0000-0002-4400-6741

Mugdha Joglekar

Western Sydney University https://orcid.org/0000-0001-5346-2266

Article

Keywords: single-cell RNA sequencing, islets, RYR2, calcium signalling, type 2 diabetes

Posted Date: November 10th, 2026

DOI: https://doi.org/10.21203/rs.3.rs-11447892/v1

License: This work is licensed under a Creative Commons Attribution 4.0 International License.
Read Full License

Additional Declarations: There is **NO** Competing Interest.

A single-cell and bulk transcriptome meta-analysis reveals RYR2 as a key biomarker and potential regulator in Type 2 Diabetes

Short Title: RYR2 dysregulation in diabetes

Hrishikesh P. Hardikar[1], Wilson K.M. Wong[1], Supreethi S Kanta, Rajveer Singh Shekhawat[2], Alexie Papanicolaou[3], Md. Shahidul Islam[4], Rashmi B. Prasad[2], Mugdha V. Joglekar[1], and Anandwardhan A. Hardikar[1]*

[1]Diabetes and Islet Biology Group, School of Medicine, Western Sydney University, Sydney, Australia
[2]Lund University Diabetes Centre, Department of Clinical Sciences, Lund University, Skåne University Hospital, Malmö, Sweden
[3]The Hawkesbury Institute for Environment, Western Sydney University, Penrith, Australia.
[4]Department of Clinical Science and Education, Södersjukhuset, Karolinska Institutet, Stockholm, Sweden; and Department of Internal Medicine, Uppsala University Hospital, Department of Medical Sciences, Uppsala University, Uppsala, Sweden

Correspondence:
Professor Anandwardhan A. Hardikar
30.2.27 David Pilgrim and Goldsmith Avenue,
Western Sydney University School of Medicine
Campbelltown, NSW 2560, Australia
Email: a.hardikar@westernsydney.edu.au
Phone: +61 488 119 772

Word count: 3171 | Abstract: 158
Figures: 7, Tables: 3, Supplementary materials: 7 (Six figures and one Excel workbook with 10 tables)

Keywords: single-cell RNA sequencing, islets, RYR2, calcium signalling, type 2 diabetes

Graphical abstract:

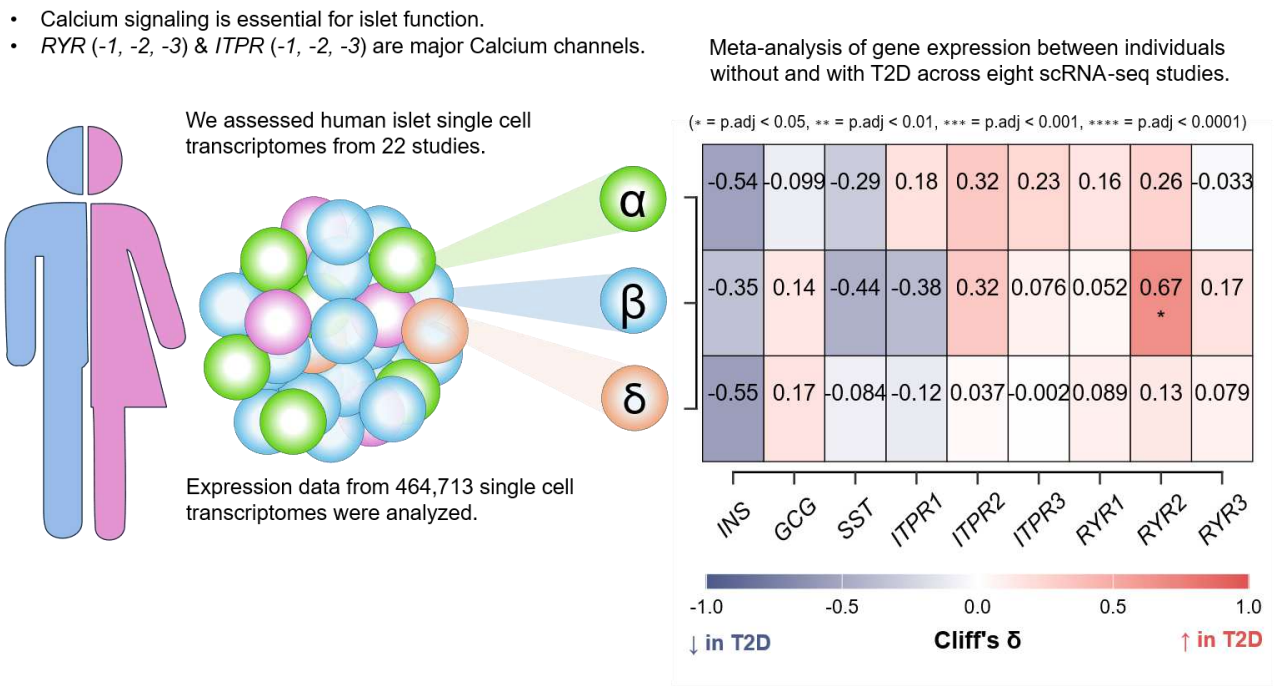

A single-cell (sc)RNA-seq meta-analysis across 464,713 islet-cell transcriptomes from n=235 human pancreas donors identified elevated β-cell RYR2 in type 2 diabetes. With a trend mapping increased RYR2 in pre-diabetes, calcium channel expression (through RYR and ITPR genes) may guide personalised strategies to reverse islet dysfunction and arrest progression from pre-diabetes to T2D.

Intracellular calcium release channels, including ryanodine receptors (RYRs) and inositol trisphosphate receptors (ITPRs), regulate calcium signalling essential for insulin secretion by pancreatic islet β-cells. However, alterations in their expression in type 2 diabetes (T2D) remain unclear. Here, we screened 1.3 million single-cell RNA sequencing transcriptomes and performed a meta-analysis of 464,713 transcriptomes from human islet α-, β-, or δ-cells across 22 independent studies from n=235 individuals with, at risk of, or without diabetes. We identified RYR2 as the predominant RYR isoform in human pancreatic islet β-cells, with significantly increased expression in T2D, compared to prediabetes and non-diabetes states. Bulk RNA sequencing of n=381 human islet samples from our own and publicly available datasets confirmed RYR2 abundance and enrichment of RYR2-212 (ENST00000714022.1) splice variant in human islets. These findings suggest that elevated β-cell RYR2 expression may contribute to islet dysfunction in T2D, identifying RYR2 as a candidate biomarker and potential therapeutic target to guide personalised strategies for diabetes management.

Islet β-cells are one of the more abundant endocrine cell types within the pancreatic islets. Upon glucose stimulation, islet β-cell membranes depolarise, leading to the opening of voltage-gated calcium channels (VGCCs) and subsequent Ca^{2+} influx. Calcium signalling is essential for regulated release of insulin into the bloodstream. Two principal types of intracellular Ca^{2+}-release channels mediate further Ca^{2+}-mobilisation from the endoplasmic reticulum (ER): the ryanodine receptors (RYRs; RYR1, RYR2, RYR3) and the inositol 1,4,5-trisphosphate receptors (ITPRs; ITPR1, ITPR2, ITPR3)[1,2]. RYR2 mainly responds to elevated cytosolic Ca^{2+} by releasing additional Ca^{2+} from the ER through a process known as calcium-induced calcium release (CICR)[3-6]. In parallel, activation of phospholipase C-linked receptors generates inositol trisphosphate (IP3), which binds to ITPRs and triggers Ca^{2+} release from the ER into the cytosol[7,8]. The resulting increase in cytosolic free Ca^{2+} concentrations ultimately triggers insulin exocytosis[9]. Human islets have been shown to contain functional[10] *RYR2* that are important in insulin secretion, and mutations in RYR2 have been associated with glucose intolerance[11]. It is well known that a defect in insulin secretion leads to β-cell dysfunction and progression to type 2 diabetes (T2D)[12,13]. However, the expression profile of RYR and ITPR gene transcripts across human islets from those without diabetes (ND), with Type 1 diabetes (T1D), pre-T2D or with T2D has not been studied at a single-cell level. We assessed whether dysfunction in CICR mediated through RYR and ITPR genes is linked with T2D.

Single-cell RNA sequencing (scRNA-seq) enables the analysis of gene expression at single-cell resolution. ScRNA-seq technology can be used to assess the abundance and proportions of *RYR* and *ITPR* gene transcripts, along with human islet (pro-) hormone transcripts (*INS, GCG, SST*). Our approach was to assess these from all available human islet scRNA-seq studies, across different types (T1D and T2D) and the entire spectrum of diabetes progression (ND, pre-T2D and T2D). Since individual studies can be biased and limited, we chose to meta-analyse existing scRNA-seq data and identify consensus across studies and from a larger

number of donors. We then analysed RYR splice forms using multicenter bulk RNA-seq data including our studies from Australia[14,15]and Europe[62]. While scRNA-seq resolves cell-type-specific expression patterns, bulk RNA sequencing offers deeper transcriptome coverage and is better suited for splice variant analysis, which are often missed by 3'-biased high-throughput scRNA-seq technologies. In mice, an alternative splice form of *Ryr2* is essential for insulin secretion in pancreatic β-cells [16,17], but such splice forms have not been characterised in human islets. In humans, tissue-specific[18]- or disease-specific[19] splice variants can provide important insights into tissue development and disease pathophysiology. Therefore, insights from both scRNA-seq and bulk-RNA-seq studies can enhance future research into potential therapeutic targets for T1D and T2D.

To address this knowledge gap, we screened 50 scRNA-seq datasets to select 22 datasets (1,304,767 transcriptomes, n=292 participants) based on inclusion/exclusion criteria (**Figure 1a**). Then, gene expression data for *RYR1, RYR2, RYR3, ITPR1, ITPR2,* and *ITPR3* genes in α-, β-, and δ-cells was obtained (464,713 transcriptomes, n=235 participants from 22 studies, after exclusion of prenatal and stem-cell-derived samples and of one dataset re-deposited in another included study; **Table 1**), and the differences in gene expression among the major islet cell types was assessed (**Table 2a, Figure 2a**). The proportion and donor information for the 22 analysed datasets using dimensionality reduction algorithms, t-distributed Stochastic Neighbour Embedding (t-SNE; used for datasets < 200,000 cells) and Uniform Manifold Approximation and Projection (UMAP; for datasets with ≥ 200,000 cells), are presented in **Figure 1b**. The relative proportions of major islet cells across the 22 studies, along with the β-cells to α-cell ratio (averaged for each cell capture method), are shown in **Figure 1c**, while the relative percentages of major islet cell types along with other cell types within each study are shown in **Figure 1d**. As expected, in individuals without diabetes, pro-hormone gene transcripts *GCG*, *INS,* and *SST* were the most abundant in α-, β-, and δ-cells, respectively. Among the ITPR genes, *ITPR1* and *ITPR3* were most highly expressed in α-cells, while *ITPR3* was the predominant isoform in both β-cells and δ-cells. *RYR2* was the most abundant RYR isoform across all three major islet cell types (**Figure 3a**).

Similarly, the three major islet cell types showed near-100% (global average across all data points) expression of their key hormone transcripts. A larger percentage of α-cells expressed *ITPR1* compared to other *ITPR* transcripts. *ITPR3* and *RYR2* were expressed in a larger percentage of β-cells, compared to other *ITPR* and *RYR* gene transcripts, respectively, which was also seen in δ-cells **(Figure 2b)**.

The percentage of cells expressing genes of interest was assessed within the major islet cells **(Table 2b, Figure 2c)**. Although all of the 22 scRNA-seq studies included sc-transcriptomes from individuals without diabetes, only eight of these studies had scRNA-seq data from more than one T2D individual/study. Only two of the 22 studies included had individuals with pre-T2D or T1D. Therefore, meta-analyses for candidate genes were performed only between ND and T2D groups. Aggregated (mean) scRNA-seq expression for each of the selected genes was compared at the donor level within each cell type across individuals with and without T2D,

within each study, to estimate the effect size (Cliff's δ). This was then used to perform a random-effects meta-analysis across all eight studies.
In pancreatic β-cells, *RYR2* was the only non-hormone transcript that showed a positive and statistically significant effect size, indicating elevated expression in individuals with T2D **(**Cliff's δ=0.67, 95% CI 0.34–0.99, Bonferroni-adjusted p=0.049; **Figure 4a)**. Since the heterogeneity was large (90%), a leave-one-out meta-analysis indicated that excluding the study GSE154126 (the only study with a negative effect) reduced the heterogeneity **(Figure 5a)**. The pooled effect remained positive for each cell capture method and did not alter significantly between them **(**p=0.4, **Supplementary Data 1)**. Analyses performed by restricting to donors with at least 5, 10, 20, or 50 β-cells, comparing donor means on the linear expression scale, or pooling the Fisher-z transformed effect sizes (atanh(δ) scale) did not change this result **(**Cliff's δ=0.59–0.93, all p<0.02; **Supplementary Data 1)**. No other gene showed significantly different expression between ND and T2D after correction for multiple comparisons; *INS* in α- and δ-cells (large and negative effect sizes) and *SST* in α- and β-cells (small/medium and negative effect sizes) were lower in T2D only before correction. All other genes showed small and statistically insignificant effects (**Figure 4c,** leave-one-out analyses for corresponding meta-analyses shown in **Supplementary figure 1a**).

The same eight studies were compared for the percentage of cells expressing each transcript. In agreement with the meta-analysis of *RYR2* expression, the percentage of β-cells expressing *RYR2* was also elevated with a large and positive effect size **(**Cliff's δ=0.65, p=0.003; Benjamini–Hochberg-adjusted p=0.04), although this did not remain significant after Bonferroni correction (p.adj=0.08; **Figure 4b)**. The heterogeneity was very large (94%), and a leave-one-out analysis indicated that removal of any study could not meaningfully reduce the heterogeneity **(Figure 5b)**. The percentage of β-cells expressing *RYR2* also remained higher in T2D when only donors with at least 5, 10, 20, or 50 β-cells were included or when stricter detection thresholds were applied **(**Cliff's δ=0.50–0.87, all p<0.01; **Supplementary Data 1)**. The percentage expression of *INS* was significantly lower in T2D across all three major islet cell types (large and negative effect sizes). The percentage of β-cells expressing *SST* was also lower in T2D (medium and negative effect size); however, none of these differences remained significant after Bonferroni correction. All other genes showed small and statistically insignificant effects (**Figure 4d,** leave-one-out analyses for corresponding meta-analyses shown in **Supplementary figure 1b**).

Of the 22 scRNA-seq studies, only two studies (GSE200044, snRNA-seq; and GSE221156, scRNA-seq) had more than one individual with pre-diabetes, and only one study had more than one individual with T1D. Both studies featured individuals with pre-diabetes and also profiled individuals with T2D. Cross-sectionally (across ND→preT2D→T2D), the expression of *RYR2* increased with disease stage in both studies (Kendall's trend test, p.adj=0.002 and 0.004), whereas the decrease in *INS* expression did not remain significant after correction (p.adj=0.09 and 0.17) **(Figure 2b)**. *RYR2* and *INS* showed a negative, strong, and significant

correlation in T2D within the study GSE200044. Across all donors, *RYR2* and *INS* were negatively correlated in both studies (GSE200044: r=−0.45, p=0.048; GSE221156: r=−0.46, p=0.001) **(Figure 3c)**.

Following assessment at the gene expression level and by cell type, we compared the proportions of major islet cells (relative to all α-, β-, and δ-cells captured per donor) assigned to α-, β-, and δ-cell types between individuals with and without diabetes. Interestingly, the proportion of α-cells was significantly higher in T2D **(**large, positive effect size, Cliff's δ=0.54, $p=2\times10^{-5}$, **Figure 4e)**, whereas the proportions of β-cells (Cliff's δ=−0.45, $p=3\times10^{-4}$) and δ-cells (Cliff's δ=−0.18, p=0.0013) were lower **(Supplementary Figure 2)**. Heterogeneity was not observed (I^2= 0%), and therefore, a leave-one-out analysis did not change this result **(Figure 5c)**.

In the only study containing more than one individual with T1D (GSE148073), only *INS* showed a significant decrease in expression in T1D compared to ND. Such a comparison for *RYR2* expression was statistically insignificant, whereas the percentage of β-cells expressing *RYR2* was lower in T1D (median 0.8% vs 2.0%; Cliff's δ=−0.91; 4 T1D and 11 ND donors), and no significant correlation was seen between INS and RYR2 expression **(Figure 5d–f)**.

Data from bulk RNA sequencing from human pancreatic islets (GSE134068, GSE152111), along with these bulk RNA-seq studies, data from publicly available studies profiling pancreatic islet cells (GSE159984) and purified pancreatic β-cells (GSE67543, GSE57973, GSE116559) were used. **Table 3** shows the details of bulk RNA-seq samples (n=463 samples from 393 donors) by condition. Of these, 149 islet samples (79 NG, 70 HG) were used for the comparison between normoglycemic and hyperglycemic individuals, and 28 purified β-cell samples (17 adult, 5 juvenile, 6 fetal) for the β-cell analyses. *RYR2* was the most abundant *RYR* transcript in both the adult pancreatic beta cells and the pancreatic islet cells **(Figure 6a)**, in agreement with the results from scRNA-seq analysis. The expression of *RYR2* was significantly higher in adult beta cells compared to fetal beta cells, but not when compared to juvenile beta cells (**Figure 6b**). However, when the expression of *RYR2* was meta-analysed between pancreatic islet cells from individuals with or without hyperglycemia or T2D, the meta-analysis did not reach statistical significance (Cliff's δ=−0.12, 95% CI −0.53 to 0.29). Leave-one-out meta-analysis showed that removal of the study GSE159984 produced a small and negative effect size **(Figure 6c)**.

Splice variant analysis revealed that more than one splice forms of *RYR2* were detected in the pancreatic beta cells as well as in pancreatic islets. Although no single transcript variant dominated pancreatic β-cells, variant *RYR2-212* (ENST00000714022.1) was significantly more abundant than any other variant of *RYR2* in the pancreatic islet cells **(Figure 6d;** other significant differences are shown in **Supplementary Data 2)**. However, it must be noted that *RYR2-212* differs from other full-length transcripts by only 178-293 bp of unique exonic

sequence. A small number of reads map uniquely to it (a median of ~1 unique read and ~150 shared reads per islet sample). Therefore, its abundance estimate relies on the probabilistic assignment of reads **(Supplementary Data 3 and 4)**. Similar results were obtained from the islet RNA-seq data through our HTL data set **(Supplementary Figure 3)**. Differential transcript variant abundance analyses between fetal and adult, or juvenile and adult beta cells did not reach statistical significance (**Figure 6e**).

When the abundance of these twelve transcript variants was meta-analysed between the normoglycemic and hyperglycemic individuals across studies, no comparison reached statistical significance, including when each variant was analysed as a fraction of total *RYR2* expression **(Figure 7; Supplementary Data 5)**. A similar pattern was observed in the HTL data set **(Supplementary Figure 3)**.

Discussion

This is the first sn/scRNA-seq meta-analysis of intracellular Ca^{2+} channels identifying differential expression of *ITPR* and *RYR* genes across human α-, β-, and δ cells. *RYR2* is the most abundantly expressed human pancreatic islet *RYR* gene transcript across all three major islet cell types, *ITPR1* is the most abundant *ITPR* gene in α-cells, and *ITPR3* is most abundant in β- and δ-cells.

Our results are in agreement with a previous study by Nordenskjöld et. al.[20] where they compared the expression of these genes in highly purified preparations of human α- and β-cells using bulk RNA sequencing performed by Blodgett et. al.[21]. This study reported *ITPR3* and *RYR2* as the most expressed *ITPR* and *RYR* transcripts in β-cells. Consistent with our findings, they reported that *ITPR1* is the most expressed *ITPR* in α-cells; however, they found *RYR1* as the most expressed *RYR* in α-cells. Blodgett et. al. reported a β-cell:α-cell ratio of ~1.42 β-cells per α-cell. In our analysis, the gross β-cell:α-cell ratio was 1.15 when calculated for studies using droplet-based cell capture, closest to this estimate. Microfluidics-based cell capture approaches showed a β-cell/α-cell ratio of 0.81, followed by FACS-based cell capture showing a β-cell/α-cell ratio of 0.44 **(Figure 1c)**. These differences may be attributable to the FACS-sorting-based scRNA-seq studies, as FACS-based cell capture methods are known to yield an underrepresentation of β-cells compared to α-cells[22]. However, studies utilising FACS-based cell capture methods contributed a small percentage of cells in our analysis (~1.5%), the majority being contributed by studies using droplet-based cell capture methods (~98%) **(Supplementary data 6)**.

Our meta-analyses identified that *RYR2* expression was consistently increased in individuals with T2D, and the percentage of β-cells expressing *RYR2* nominally increased in T2D. No other calcium release channel displayed such an elevation in expression. On the other hand, *INS* and *SST* showed negative effects in terms of gene expression or percentage of cells expressing the gene, implying an overall lower abundance (expression) in T2D, although not significant after correction. Lower *INS* in α- and δ-cells may partly reflect ambient *INS* transcripts, as *INS* was also lower in exocrine cells from individuals with T2D **(Supplementary Data 1)**. *GCG*

transcripts, however, did not show any significant change in individuals with T2D **(Figure 4c, d)**, which may be explained by the significant increase in the proportion of α-cells in individuals with T2D (**Figure 4e**). De-differentiation of pancreatic β-cells into polyhormonal cells or α-like cells has been reported[23-25]. Although the proportion of β-cells was lower in individuals with T2D **(Supplementary Figure 2**), the cross-sectional nature of these studies does not allow the assessment of longitudinal changes in cellular identity.

It remains unclear if increased *RYR2* is a cause or effect of T2D based on these cross-sectional studies. We found that across ND→preT2D→T2D, *RYR2* and *INS* were negatively correlated. In T2D, *INS* expression was at its lowest, whilst *RYR2* was at its highest **(Figure 3c)**. Leaky RyRs can cause leakage of Ca^{2+} ions from the ER, which requires additional, futile ATP expenditure to restore the ER-Ca^{2+} store. Such efflux of Ca^{2+} from the ER is associated with β-cell death[26]. Indeed, increased expression/activation of *RyR1/RyR2,* respectively, is associated with efflux of ER-Ca^{2+} in cell lines and rodents [27-29]. While the evidence around the association of *RYR2* upregulation and ER stress in humans remains under-investigated, our analysis identifies increased abundance of *RYR2* in human β-cell transcriptomes in T2D. This increased expression of *RYR2* in the β-cells may be associated with increased vulnerability to damage, as suggested by previous reports linking *RYR2* alterations to Ca^{2+} leakage, ER Ca^{2+} store depletion, ER stress, and apoptosis[11,27,28,30]. The reduced expression of non-lineage-defining genes in T2D cells could also indicate a state of cellular stress (e.g., due to reduced number of cells and/or increased demand for hormone secretion), wherein the cells prioritise the transcription of their primary/lineage-defining gene in favour of other transcripts.

Bulk RNA-seq analysis revealed multiple *RYR2* isoforms are present in sequencing data from pancreatic β-cells and pancreatic islets. Of the twelve *RYR2* transcript variants, *RYR2-205, -206, -207, -209, -210,* and *-212* were detected in pancreatic β-cells and pancreatic islet cells **(Figure 6d and Supplementary Figure 3)**. The canonical *RYR2* transcript*,* the *RYR2-201* (ENST00000366574.7) variant, which is predominantly expressed in cardiac tissue[31,32] showed little to no expression in these samples. Instead, *RYR2-212* (ENST00000714022.1) was identified as the most abundantly expressed variant in all three public islet datasets **(**43–47% of *RYR2* expression; **Supplementary Data 7)**, whereas it was the second-most abundant splice variant in the HTL dataset and not consistently the most abundant in purified β-cells. This transcript has 89 exons, with 86 (exons 4-88) translated to a protein of 4312 amino acid residues, as compared to the cardiac-type *RYR2-201,* which has 105 coding exons and encodes a protein sequence of 4967 amino acids. These findings are consistent with the presence of a distinct *RYR2* splice variant in pancreatic tissue, as observed in mice[16,17]. Because *RYR2-212* shares most of its sequence with other full-length transcript variants, its abundance estimates rely on the probabilistic assignment of shared reads **(Supplementary Figure 4)**, and techniques generating direct evidence (e.g., splice-junction reads or long-read sequencing) will be required to confirm the presence of this isoform in pancreatic islets. Subtle differences among studies in the abundance of individual transcript variants may reflect differences in study populations. Further research is needed to clarify the functional significance of alternative *RYR2* splice forms in pancreatic islets.

Whilst scRNA-seq data meta-analysis is a strength of this study, there are few limitations. This technique is subject to 3' bias and limited detection of low-expressed genes, which can result in under-representation or omission of genes with low copy numbers per cell compared to bulk RNA-seq. Additionally, scRNA-seq results can be influenced by methodological differences, complicating multi-study data integration. The zero-heavy and non-continuous nature of scRNA-seq datasets, particularly for low-expressed genes, necessitates careful statistical modelling and batch-effect correction, as reflected by the substantial inter-study heterogeneity observed in our meta-analyses. As only normalised expression of the candidate transcripts was available, ambient RNA could not be removed; *RYR2* also tended to be higher in exocrine cells from individuals with T2D, albeit more weakly than in β-cells **(Supplementary Data 1)**, so a contribution of global differences in detection cannot be fully excluded. To address these challenges, we employed non-parametric meta-analytical approaches to examine gene expression patterns between ND and T2D. This approach enabled us to identify *RYR2* as a key target. We confirmed that *RYR2* is the most abundant *RYR* isoform in both purified β-cells and pancreatic islet cells using bulk RNA-seq; however, we were unable to validate the increase in *RYR2* expression in T2D using bulk RNA-seq, which was not explained by dilution of the β-cell signal by non-β-cell transcripts alone **(Supplementary Figure 5)**, as adjusting for β-cell and exocrine marker content did not change the result **(Supplementary Data 8)**; differences between cohorts and in the definition of glycemic status may contribute. Future studies should focus on elucidating the molecular mechanisms that lead to increased *RYR2* expression in β-cells during various stages of progressive insulin secretion impairment in T2D. Understanding these mechanisms could provide valuable insights into the pathogenesis of T2D and potentially reveal new therapeutic targets to retard or prevent the progression to T2D.

Methods

Analysis of publicly available scRNA-seq data

A total of 50 publicly accessible scRNA-seq transcriptomes were identified for human islet datasets (**Figure 1a**), and scRNA-seq data from major (α-, β-, and δ-) islet cells that were not exposed to any drugs or molecules were eligible, from a total of 1,304,767 transcriptomes across n=292 donors. Transcriptomes from cell types other than major islet cells or from conditions other than non-diabetic (ND), pre-T2D, T1D, and T2D were excluded from the analysis. Transcriptomes from prenatal pancreas (GSE197064, OMIX001616) and from stem-cell-derived cells (SCP1526 lines H1 and CyT49) were also excluded (7,057 transcriptomes, 18 donors), as was study GSE83139, whose cells were re-deposited as part of GSE154126 (310 transcriptomes, 9 donor samples), leaving 464,713 transcriptomes from 235 donors across 22 studies. The number of transcriptomes from each cell type that passed the inclusion criteria from each cell type by condition, and the number of donors for each condition are shown in **Table 1**. For the representation of the included datasets (**Figure 1b)**, dimensionality reduction was performed within the Talk2Data platform (t-Stochastic Neighbor Embedding (t-SNE) was used for datasets <200,000 cells, and Uniform Manifold Approximation and Projection (UMAP) was used for datasets with ≥ 200,000 cells).

Study methods

Our combined study set (a total of 25 datasets) features a high diversity, owing to (but not limited to) the factors listed below:

1. Study approach: scRNA-seq (23/25) and snRNA-seq (2/25)
2. Cell capture methods: droplet-based (15/25), fluorescence-activated cell sorting (FACS, 6/25), and microfluidic chip-based (4/25)
3. Technology: 10X Genomics (13/25), SmartSeq-2 (6/25), CEL-Seq-2 (2/25), SMART-methods (4/25), inDrop (1/25)
4. Country of origin: USA (13/25), CAN (2/25), GER (2/25), NED (2/25), SWE (2/25), CHE (1/25), CHN (1/25), FIN (1/25), GBR (1/25)

Figure 1c shows the relative percentages of major islet cells across the 22 studies, along with the β-cells to α-cell ratio (averaged for each cell capture method). **Figure 1d** shows relative percentages of major islet cell types along with other cell types within each study.

Database search and accession

Based on the inclusion/exclusion criteria (**Figure 1a**), we selected 25 of the 50 scRNA-seq datasets, and obtained the standardized metadata (cell type, condition, donor/subject ID), from public datasets using the Talk2data tool from BioTuring [33]:
E_MTAB_5061 [34], GSE101207 [35], GSE114297 [36-38], GSE148073 [39], GSE150724 [40,41], GSE153855 [22], GSE154126 [42], GSE183568 [43], GSE197064 [44], GSE198623 [45], GSE200044 [46], GSE201333 [47], GSE221156 [48], GSE269204 [49], GSE81076 [50], GSE81547 [51], GSE81608 [52], GSE83139 [53], GSE84133 [54], GSE85241 [55], GSE86473 [56], OMIX001616 [57], PMID33212097 [58], PMID35081145 [59], SCP1526

[60]. GSE124742 was excluded at the screening stage as the cell numbers available through Talk2Data did not match those reported by the authors. Donor overlaps across different datasets were avoided by assessing for matching donor IDs, sample accessions, demographic fields, and isolation centre identifiers where available. For the representation of the included datasets **(Figure 1b)**, dimensionality reduction was performed using t-distributed Stochastic Neighbour Embedding (t-SNE) for datasets < 200,000 transcriptomes, and Uniform Manifold Approximation and Projection (UMAP) was used for datasets with ≥ 200,000 transcriptomes.

Bulk RNA-seq was carried out on human islet cells as described earlier [14,18,61,62], and data were uploaded to NCBI (GSE134068 [14], GSE152111 [15]). Along with our bulk RNA-seq data, we also downloaded and analysed data from other publicly available studies: GSE116559 [63], GSE57973 [64], GSE67543 [21], GSE159984 [65]. Independent analyses were carried out in the HTL dataset to assess the similarity/variability across ethnically/contextually diverse cohorts. Human genome primary assembly (GRCh38.p14) and the corresponding annotation were downloaded from GENCODE (release 48, [66]).

scRNA-seq analyses

Single-cell RNA-seq can be greatly influenced by the methodology, and as such, comparison of data from different studies can be challenging. Therefore, we adopted an evidence combination method: Gene expression data from single cells were aggregated (mean) at the donor level. For comparison of gene expression **(**expression values or percent expression, **Figure 3a, Figure 2)**, donor-level expression data were compared within the study using paired non-parametric tests (pairwise, paired Wilcoxon Signed-Rank Tests), and the standardised, signed test statistics (Z) were combined using Stouffer's method [67] to generate a combined Z statistic and the associated p-value. These p-values were then adjusted for multiple comparisons using the Bonferroni correction.

For comparison between individuals without and with T2D across studies, random-effects meta-analyses were conducted.

Bulk RNA-seq analyses

The NCBI SRA [68] toolkit v. 3.0.3 was used to download the sequencing data. FastQC v. 0.12.1 [69] and MultiQC (v. 1.28) [70] were used to detect adapter content and low-quality read content, which were removed using Cutadapt [71]. Clean reads were mapped onto the human genome primary assembly (GRCh38.p14) from the GENCODE release 48 [66] using the STAR aligner v. 2.7.11b [72], and the transcript-level quantifications were generated using Salmon v. 1.10.3 [73].

For evidence synthesis, gene-level or transcript-level quantifications were compared within a study using paired non-parametric tests, followed by evidence combination (as discussed previously). For comparison of individuals without or with hyperglycemia/T2D, random-effects meta-analyses were conducted.

Data analysis and visualisation were performed using the R programming language (v. 4.6.0 "Because it was there") [74]. The data were imported into RStudio Desktop (v. 2026.04.0+526)

[75]. For the import, analysis, visualisation, and export of the data, the cited R packages were used [76-95].

Statistical analysis and power

All scRNA-seq comparisons were performed on donor-level aggregates to avoid pseudoreplication. For each donor within each study, we computed the mean normalized expression and the percentage of cells expressing each transcript, separately for each of the three islet cell types analysed. Cell-type comparisons in non-diabetic donors were made on paired donor-level values using the Wilcoxon signed-rank test, and the standardised signed test statistics were combined across studies by Stouffer's method; resulting P values were Bonferroni-adjusted across all transcript and cell-type comparisons.

Between-disease comparisons were made only for ND and T2D groups, because eight of the 22 studies contained scRNA-seq data from more than one T2D donor, whereas only two studies contained more than one pre-T2D or T1D donor. Within each study, donor-level expression values (or percentage of expressing cells) were compared between ND and T2D donors using Cliff's δ, an ordinal, distribution-free effect-size estimator appropriate to zero-inflated single-cell data, with variance estimated by the standard asymptotic approximation.

Effect sizes were pooled across studies using random-effects meta-analysis, with restricted maximum-likelihood (REML) estimation of the between-study variance and Hartung–Knapp adjusted confidence intervals and tests (Paule–Mandel estimation was used where REML did not converge); 95% prediction intervals are reported alongside pooled estimates. Cell-type composition was compared as the proportion of α-, β-, and δ-cells among all major islet cells captured per donor. A leave-one-out meta-analysis and subgroup analyses by cell-capture method (with a test for subgroup differences), restriction to donors with at least 5, 10, 20, or 50 β-cells, alternative expression scales and detection thresholds, and a negative control in exocrine cells are reported as sensitivity analyses **(leave-one-out: Figure 5 and Supplementary figure 1; all others: Supplementary Figure 6 and Supplementary Data 1)**.

The ND vs T2D meta-analysis of β-cell *RYR2* expression combined eight studies comprising 122 donors (70 ND, 52 T2D) and 97,655 β-cell transcriptomes; no a priori power calculation was performed, and the precision of each estimate is conveyed by its confidence and prediction intervals. Correlations between *INS* and *RYR2* expression were assessed by Pearson's r on donor-level values, within each disease stage and across all donors of each study; trends in donor-level expression across ND, preT2D, and T2D were tested by Kendall's τ between expression and disease stage (coded 0, 1, 2). All P values are two-sided and adjusted for multiple comparisons by the Bonferroni method unless stated; Benjamini–Hochberg false discovery rate (FDR)-adjusted values are additionally reported where stated.

Data availability

Sequencing data for all scRNA-seq and bulk RNA-seq datasets are publicly available. Donor data were accessed through the BioTuring Talk2Data interface. Specific scripts for analyses and donor data for GSE134068 and GSE152111 are available upon request or through GitHub/isletbiology. The HTL data is available upon request at the European Genome-phenome Archive (EGA; https://ega-archive.org/) under the following accession numbers: EGAS00001004042 [https://ega-archive.org/studies/EGAS00001004042].

Statement on the use of Artificial Intelligence-assisted technologies

Grammarly® was used for maintaining the language and grammatical accuracy of the manuscript. AI was not utilised for writing the manuscript prose; the lead/corresponding authors take responsibility for the analysis. AAH takes responsibility for all data and the submission of this manuscript.

Acknowledgements

HPH was supported through a post-graduate scholarship from Western Sydney University. His research was supported by the Commonwealth through an Australian Government Research Training Program Scholarship [DOI: https://doi.org/10.82133/C42F-K220]. WKMW is supported through a Breakthrough T1D USA Advanced postdoctoral researcher fellowship (3-APF-2026-1878-A-N). SK is an MD student and has been supported through the summer research scholarship program at Western Sydney University Faculty of Health, School of Medicine. RSS and RBP have been supported through Lund University, Malmo, Sweden and MSI is supported through Karolinska Institute, Sweden. AP is supported through Hawkesbury Institute, Western Sydney University and MVJ and AAH acknowledge the support through the Ainsworth Medical Research Foundation, Western Sydney University, Sydney, Australia.

Author contribution:

HPH, WKMW, SK, RSS carried out the analysis presented in this manuscript. AP, MSI, RBP, MVJ, and AAH assessed these analyses and provided project supervision. HPH led most analyses and wrote the first draft and revised drafts with AAH. All authors read the drafts, amended the drafts and agreed on their contributions.

References

1 Santulli, G., Nakashima, R., Yuan, Q. & Marks, A. R. Intracellular calcium release channels: an update. *J Physiol* **595**, 3041-3051 (2017). https://doi.org/10.1113/JP272781

2 Graves, T. K. & Hinkle, P. M. Ca(2+)-induced Ca(2+) release in the pancreatic beta-cell: direct evidence of endoplasmic reticulum Ca(2+) release. *Endocrinology* **144**, 3565-3574 (2003). https://doi.org/10.1210/en.2002-0104

3 Islam, M. S., Rorsman, P. & Berggren, P. O. Ca(2+)-induced Ca2+ release in insulin-secreting cells. *FEBS Lett* **296**, 287-291 (1992). https://doi.org/10.1016/0014-5793(92)80306-2

4 Islam, M. S. Calcium signaling in the islets. *Adv Exp Med Biol* **654**, 235-259 (2010). https://doi.org/10.1007/978-90-481-3271-3_11

5 Islam, M. S. The ryanodine receptor calcium channel of beta-cells: molecular regulation and physiological significance. *Diabetes* **51**, 1299-1309 (2002). https://doi.org/10.2337/diabetes.51.5.1299

6 Holz, G. G., Leech, C. A., Heller, R. S., Castonguay, M. & Habener, J. F. cAMP-dependent mobilization of intracellular Ca2+ stores by activation of ryanodine receptors in pancreatic beta-cells. A Ca2+ signaling system stimulated by the insulinotropic hormone glucagon-like peptide-1-(7-37). *J Biol Chem* **274**, 14147-14156 (1999). https://doi.org/10.1074/jbc.274.20.14147

7 Gustafsson, A. J. & Islam, M. S. [Cellular calcium ion signalling--from basic research to benefits for patients]. *Lakartidningen* **102**, 3214-3219 (2005).

8 Gromada, J., Frokjaer-Jensen, J. & Dissing, S. Glucose stimulates voltage- and calcium-dependent inositol trisphosphate production and intracellular calcium mobilization in insulin-secreting beta TC3 cells. *Biochem J* **314 (Pt 1)**, 339-345 (1996). https://doi.org/10.1042/bj3140339

9 Fu, Z., Gilbert, E. R. & Liu, D. Regulation of insulin synthesis and secretion and pancreatic Beta-cell dysfunction in diabetes. *Curr Diabetes Rev* **9**, 25-53 (2013).

10 Johnson, J. D., Kuang, S., Misler, S. & Polonsky, K. S. Ryanodine receptors in human pancreatic beta cells: localization and effects on insulin secretion. *FASEB J* **18**, 878-880 (2004). https://doi.org/10.1096/fj.03-1280fje

11 Santulli, G. *et al.* Calcium release channel RyR2 regulates insulin release and glucose homeostasis. *J Clin Invest* **125**, 1968-1978 (2015). https://doi.org/10.1172/JCI79273

12 Kahn, S. E. Clinical review 135: The importance of beta-cell failure in the development and progression of type 2 diabetes. *J Clin Endocrinol Metab* **86**, 4047-4058 (2001). https://doi.org/10.1210/jcem.86.9.7713

13 Ludwig, D. S. *et al.* The carbohydrate-insulin model: a physiological perspective on the obesity pandemic. *Am J Clin Nutr* **114**, 1873-1885 (2021). https://doi.org/10.1093/ajcn/nqab270

14 Wong, W. K. M. *et al.* Machine learning workflows identify a microRNA signature of insulin transcription in human tissues. *iScience* **24**, 102379 (2021). https://doi.org/10.1016/j.isci.2021.102379

15 Wong, W. K., Joglekar, M. V., Chew, Y. V., Hawthorne, W. J. & Hardikar, A. A. (NCBI GEO, 2021).

16 Takasawa, S. *et al.* A novel ryanodine receptor expressed in pancreatic islets by alternative splicing from type 2 ryanodine receptor gene. *Biochem Biophys Res Commun* **397**, 140-145 (2010). https://doi.org/10.1016/j.bbrc.2010.05.051

17 Okamoto, H., Takasawa, S. & Yamamoto, Y. From insulin synthesis to secretion: Alternative splicing of type 2 ryanodine receptor gene is essential for insulin secretion in pancreatic beta cells. *Int J Biochem Cell Biol* **91**, 176-183 (2017). https://doi.org/10.1016/j.biocel.2017.07.009
18 Joglekar, M. V. *et al.* A Pro-Endocrine Pancreatic Islet Transcriptional Program Established During Development Is Retained in Human Gallbladder Epithelial Cells. *Cell Mol Gastroenterol Hepatol* **13**, 1530-1553 e1534 (2022). https://doi.org/10.1016/j.jcmgh.2022.01.008
19 van Tienhoven, R. *et al.* Presence of immunogenic alternatively spliced insulin gene product in human pancreatic delta cells. *Diabetologia* **66**, 884-896 (2023). https://doi.org/10.1007/s00125-023-05882-y
20 Nordenskjold, F., Andersson, B. & Islam, M. S. Expression of the Inositol 1,4,5-Trisphosphate Receptor and the Ryanodine Receptor Ca(2+)-Release Channels in the Beta-Cells and Alpha-Cells of the Human Islets of Langerhans. *Adv Exp Med Biol* **1131**, 271-279 (2020). https://doi.org/10.1007/978-3-030-12457-1_11
21 Blodgett, D. M. *et al.* Novel Observations From Next-Generation RNA Sequencing of Highly Purified Human Adult and Fetal Islet Cell Subsets. *Diabetes* **64**, 3172-3181 (2015). https://doi.org/10.2337/db15-0039
22 Ngara, M. & Wierup, N. Lessons from single-cell RNA sequencing of human islets. *Diabetologia* **65**, 1241-1250 (2022). https://doi.org/10.1007/s00125-022-05699-1
23 Talchai, C., Xuan, S., Lin, H. V., Sussel, L. & Accili, D. Pancreatic beta cell dedifferentiation as a mechanism of diabetic beta cell failure. *Cell* **150**, 1223-1234 (2012). https://doi.org/10.1016/j.cell.2012.07.029
24 Cinti, F. *et al.* Evidence of beta-Cell Dedifferentiation in Human Type 2 Diabetes. *J Clin Endocrinol Metab* **101**, 1044-1054 (2016). https://doi.org/10.1210/jc.2015-2860
25 Spijker, H. S. *et al.* Conversion of mature human beta-cells into glucagon-producing alpha-cells. *Diabetes* **62**, 2471-2480 (2013). https://doi.org/10.2337/db12-1001
26 Hara, T. *et al.* Calcium efflux from the endoplasmic reticulum leads to beta-cell death. *Endocrinology* **155**, 758-768 (2014). https://doi.org/10.1210/en.2013-1519
27 Zhang, I. X. *et al.* ER stress increases expression of intracellular calcium channel RyR1 to modify Ca(2+) homeostasis in pancreatic beta cells. *J Biol Chem* **299**, 105065 (2023). https://doi.org/10.1016/j.jbc.2023.105065
28 Yamamoto, W. R. *et al.* Endoplasmic reticulum stress alters ryanodine receptor function in the murine pancreatic beta cell. *J Biol Chem* **294**, 168-181 (2019). https://doi.org/10.1074/jbc.RA118.005683
29 Islam, M. S. Ryanodine Receptors in Islet Cell Function: Calcium Signaling, Hormone Secretion, and Diabetes. *Cells* **14** (2025). https://doi.org/10.3390/cells14100690
30 Luciani, D. S. *et al.* Roles of IP3R and RyR Ca2+ channels in endoplasmic reticulum stress and beta-cell death. *Diabetes* **58**, 422-432 (2009). https://doi.org/10.2337/db07-1762
31 Uhlen, M. *et al.* Proteomics. Tissue-based map of the human proteome. *Science* **347**, 1260419 (2015). https://doi.org/10.1126/science.1260419
32 *Human Protein Atlas*, <proteinatlas.org> (
33 (BioTuring, Santiago, CA, USA).

34 Segerstolpe, A. *et al.* Single-Cell Transcriptome Profiling of Human Pancreatic Islets in Health and Type 2 Diabetes. *Cell Metab* **24**, 593-607 (2016). https://doi.org/10.1016/j.cmet.2016.08.020
35 Fang, Z. *et al.* Single-Cell Heterogeneity Analysis and CRISPR Screen Identify Key beta-Cell-Specific Disease Genes. *Cell Rep* **26**, 3132-3144 e3137 (2019). https://doi.org/10.1016/j.celrep.2019.02.043
36 Xin, Y. *et al.* Pseudotime Ordering of Single Human beta-Cells Reveals States of Insulin Production and Unfolded Protein Response. *Diabetes* **67**, 1783-1794 (2018). https://doi.org/10.2337/db18-0365
37 Dominguez Gutierrez, G. *et al.* Gene Signature of the Human Pancreatic epsilon Cell. *Endocrinology* **159**, 4023-4032 (2018). https://doi.org/10.1210/en.2018-00833
38 Sui, L. *et al.* Reduced replication fork speed promotes pancreatic endocrine differentiation and controls graft size. *JCI Insight* **6** (2021). https://doi.org/10.1172/jci.insight.141553
39 Fasolino, M. *et al.* Single-cell multi-omics analysis of human pancreatic islets reveals novel cellular states in type 1 diabetes. *Nat Metab* **4**, 284-299 (2022). https://doi.org/10.1038/s42255-022-00531-x
40 Perez-Frances, M. *et al.* Pancreatic Ppy-expressing gamma-cells display mixed phenotypic traits and the adaptive plasticity to engage insulin production. *Nat Commun* **12**, 4458 (2021). https://doi.org/10.1038/s41467-021-24788-0
41 Perez-Frances, M. *et al.* Author Correction: Pancreatic Ppy-expressing gamma-cells display mixed phenotypic traits and the adaptive plasticity to engage insulin production. *Nat Commun* **12**, 5783 (2021). https://doi.org/10.1038/s41467-021-26062-9
42 Avrahami, D. *et al.* Single-cell transcriptomics of human islet ontogeny defines the molecular basis of beta-cell dedifferentiation in T2D. *Mol Metab* **42**, 101057 (2020). https://doi.org/10.1016/j.molmet.2020.101057
43 Shrestha, S. *et al.* Combinatorial transcription factor profiles predict mature and functional human islet alpha and beta cells. *JCI Insight* **6** (2021). https://doi.org/10.1172/jci.insight.151621
44 Olaniru, O. E. *et al.* Single-cell transcriptomic and spatial landscapes of the developing human pancreas. *Cell Metab* **35**, 184-199 e185 (2023). https://doi.org/10.1016/j.cmet.2022.11.009
45 Tritschler, S. *et al.* A transcriptional cross species map of pancreatic islet cells. *Mol Metab* **66**, 101595 (2022). https://doi.org/10.1016/j.molmet.2022.101595
46 Wang, G. *et al.* Integrating genetics with single-cell multiomic measurements across disease states identifies mechanisms of beta cell dysfunction in type 2 diabetes. *Nat Genet* **55**, 984-994 (2023). https://doi.org/10.1038/s41588-023-01397-9
47 Tabula Sapiens, C. *et al.* The Tabula Sapiens: A multiple-organ, single-cell transcriptomic atlas of humans. *Science* **376**, eabl4896 (2022). https://doi.org/10.1126/science.abl4896
48 Bandesh, K. *et al.* Single-cell decoding of human islet cell type-specific alterations in type 2 diabetes reveals converging genetic- and state-driven beta -cell gene expression defects. *bioRxiv* (2025). https://doi.org/10.1101/2025.01.17.633590
49 Ewald, J. D. *et al.* HumanIslets: An integrated platform for human islet data access and analysis. *bioRxiv* (2024). https://doi.org/10.1101/2024.06.19.599613

50 Grun, D. *et al.* De Novo Prediction of Stem Cell Identity using Single-Cell Transcriptome Data. *Cell Stem Cell* **19**, 266-277 (2016). https://doi.org/10.1016/j.stem.2016.05.010
51 Enge, M. *et al.* Single-Cell Analysis of Human Pancreas Reveals Transcriptional Signatures of Aging and Somatic Mutation Patterns. *Cell* **171**, 321-330 e314 (2017). https://doi.org/10.1016/j.cell.2017.09.004
52 Xin, Y. *et al.* RNA Sequencing of Single Human Islet Cells Reveals Type 2 Diabetes Genes. *Cell Metab* **24**, 608-615 (2016). https://doi.org/10.1016/j.cmet.2016.08.018
53 Wang, Y. J. *et al.* Single-Cell Transcriptomics of the Human Endocrine Pancreas. *Diabetes* **65**, 3028-3038 (2016). https://doi.org/10.2337/db16-0405
54 Baron, M. *et al.* A Single-Cell Transcriptomic Map of the Human and Mouse Pancreas Reveals Inter- and Intra-cell Population Structure. *Cell Syst* **3**, 346-360 e344 (2016). https://doi.org/10.1016/j.cels.2016.08.011
55 Muraro, M. J. *et al.* A Single-Cell Transcriptome Atlas of the Human Pancreas. *Cell Syst* **3**, 385-394 e383 (2016). https://doi.org/10.1016/j.cels.2016.09.002
56 Lawlor, N. *et al.* Single-cell transcriptomes identify human islet cell signatures and reveal cell-type-specific expression changes in type 2 diabetes. *Genome Res* **27**, 208-222 (2017). https://doi.org/10.1101/gr.212720.116
57 Ma, Z. *et al.* Deciphering early human pancreas development at the single-cell level. *Nat Commun* **14**, 5354 (2023). https://doi.org/10.1038/s41467-023-40893-8
58 Tosti, L. *et al.* Single-Nucleus and In Situ RNA-Sequencing Reveal Cell Topographies in the Human Pancreas. *Gastroenterology* **160**, 1330-1344 e1311 (2021). https://doi.org/10.1053/j.gastro.2020.11.010
59 Marquez-Curtis, L. A. *et al.* Cryopreservation and post-thaw characterization of dissociated human islet cells. *PLoS One* **17**, e0263005 (2022). https://doi.org/10.1371/journal.pone.0263005
60 Balboa, D. *et al.* Functional, metabolic and transcriptional maturation of human pancreatic islets derived from stem cells. *Nat Biotechnol* **40**, 1042-1055 (2022). https://doi.org/10.1038/s41587-022-01219-z
61 Wong, W. K. *et al.* The long noncoding RNA MALAT1 predicts human pancreatic islet isolation quality. *JCI Insight* **5** (2019). https://doi.org/10.1172/jci.insight.129299
62 Asplund, O. *et al.* Islet Gene View-a tool to facilitate islet research. *Life Sci Alliance* **5** (2022). https://doi.org/10.26508/lsa.202201376
63 Haliyur, R. *et al.* Human islets expressing HNF1A variant have defective beta cell transcriptional regulatory networks. *J Clin Invest* **129**, 246-251 (2019). https://doi.org/10.1172/JCI121994
64 Arda, H. E. *et al.* Age-Dependent Pancreatic Gene Regulation Reveals Mechanisms Governing Human beta Cell Function. *Cell Metab* **23**, 909-920 (2016). https://doi.org/10.1016/j.cmet.2016.04.002
65 Marselli, L. *et al.* Persistent or Transient Human beta Cell Dysfunction Induced by Metabolic Stress: Specific Signatures and Shared Gene Expression with Type 2 Diabetes. *Cell Rep* **33**, 108466 (2020). https://doi.org/10.1016/j.celrep.2020.108466
66 Mudge, J. M. *et al.* GENCODE 2025: reference gene annotation for human and mouse. *Nucleic Acids Res* **53**, D966-D975 (2025). https://doi.org/10.1093/nar/gkae1078

67 Stouffer, S. A., Suchman, E. A., DeVinny, L. C., Star, S. A. & Williams, R. M. *The American Soldier: Adjustment During Army Life (Vol. 1)*. Vol. 1 (Princeton, NJ: Princeton University Press, 1949).
68 Sayers, E. W. *et al.* Database resources of the National Center for Biotechnology Information in 2025. *Nucleic Acids Res* **53**, D20-D29 (2025). https://doi.org/10.1093/nar/gkae979
69 FastQC: A quality control tool for high throughput sequence data. v. 0.12.1.
70 Ewels, P., Magnusson, M., Lundin, S. & Kaller, M. MultiQC: summarize analysis results for multiple tools and samples in a single report. *Bioinformatics* **32**, 3047-3048 (2016). https://doi.org/10.1093/bioinformatics/btw354
71 Cutadapt removes adapter sequences from high-throughput sequencing reads v. 1.28 (EMBnet.journal, 2011).
72 Dobin, A. *et al.* STAR: ultrafast universal RNA-seq aligner. *Bioinformatics* **29**, 15-21 (2013). https://doi.org/10.1093/bioinformatics/bts635
73 Patro, R., Duggal, G., Love, M. I., Irizarry, R. A. & Kingsford, C. Salmon provides fast and bias-aware quantification of transcript expression. *Nat Methods* **14**, 417-419 (2017). https://doi.org/10.1038/nmeth.4197
74 R: A Language and Environment for Statistical Computing v. 4.6.0 "Because it was There" (R Foundation for Statistical Computing, Vienna, Austria, 2023).
75 RStudio: Integrated Development Environment for R v. 2026.04.0+526 (Posit Software, PBC, Boston, MA, 2023).
76 openxlsx2: Read, Write nd Edite 'xlsx' Files. v. 1.25. (2026).
77 Campitelli, E. ggnewscale: Multiple Fill and Colour Scales in 'ggplot2'. (2025). https://doi.org/10.32614/CRAN.package.ggnewscale
78 Chen, Y., Chen, L., Lun, A. T. L., Baldoni, P. L. & Smyth, G. K. edgeR v4: powerful differential analysis of sequencing data with expanded functionality and improved support for small counts and larger datasets. *Nucleic Acids Research* **53**, gkaf018 (2025). https://doi.org/10.1093/nar/gkaf018
79 ggprism: A 'ggplot2' Extension Inspired by 'GraphPad Prism' v. 1.0.4 (2022).
80 Hester, J., Wickham, H. & Bryan, J. vroom: Read and Write Rectangular Text Data Quickly. (2026). https://doi.org/doi:10.32614/CRAN.package.vroom
81 Hothorn, T., Hornik, K., van de Wiel, M. & Zeileis, A. Implementing a class of permutation tests: The coin package. *Journal of Statistical Software* **28(8)**, 1-23 (2008). https://doi.org/10.18637/jss.v028.i08
82 rstatix: Pipe-Friendly Framework for Basic Statistical Tests v. 0.7.2 (2023).
83 Lawrence, M., Gentleman, R. & Carey, V. rtracklayer: an {R} package for interfacing with genome browsers. *Bioinformatics* **25**, 1841-1842 (2009). https://doi.org/10.1093/bioinformatics/btp328
84 Love, M. I. *et al.* Tximeta: Reference sequence checksums for provenance identification in RNA-seq. *PLOS Computational Biology* **16**, e1007664 (2020). https://doi.org/10.1371/journal.pcbi.1007664
85 ggforce: Accelerating 'ggplot2' v. 0.4.1 (2022).
86 patchwork: The Composer of Plots v. 1.3.2 (2025).
87 ggrastr: Rasterize Layers for 'ggplot2' v. 1.0.2 (2023).
88 Soneson, C., Love, M. I. & Robinson, M. D. Differential analyses for RNA-seq: transcript-level estimates improve gene-level inferences. *F1000Research* **4** (2015). https://doi.org/10.12688/f1000research.7563.1
89 effsize: Efficient Effect Size Computation v. 0.8.1 (2020).

90 Viechtbauer, W. Conducting meta-analyses in R with the metafor package. *Journal of Statistical Software* **36(3)**, 1-48 (2010). https://doi.org/10.18637/jss.v036.i03
91 purrr: Functional Programming Tools v. 1.2.1 (2026).
92 scales: Scale Functions for Visualization (2025).
93 Welcome to the tidyverse (Journal of Open Source Software, 4(43), 1686, 2019).
94 ggtext: Improved Text Rendering Support for 'ggplot2' v. 0.1.2 (2022).
95 kableExtra: Construct Complex Table with 'kable' and Pipe Syntax v. 1.4.0 (2024).

Table 1: Number of single-cell RNA-seq transcriptomes and donors across the 22 analysed datasets

	ND	**T1D**	**preT2D**	**T2D**	**Total**
α	132,320	1,727	37,229	49,459	220,735
β	128,937	1,071	46,068	39,457	215,533
δ	18,355	193	4,655	5,242	28,445
Total transcriptomes (n)	279,612	2,991	87,952	94,158	464,713
Donors (N)	154	5	22	54	235

Table 2a: Comparison of major islet cell types in terms of the candidate gene expression

Gene transcript	**Comparisons between cell types**
GCG	α-cells > β-cells, α-cells > δ-cells
INS	β-cells > δ-cells > α-cells
SST	δ-cells > β-cells > α-cells
ITPR1	α-cells > δ cells > β cells
ITPR2	β-cells > δ-cells > α-cells
ITPR3	β-cells > δ-cells > α-cells
RYR1	δ-cells > α-cells, δ-cells > β-cells
RYR2	β-cells > α-cells, δ-cells > α-cells
RYR3	No comparison reached statistical significance

Table 2b: Comparison of the percentage of major islet cells expressing GCG, INS, SST, ITPR1-3, and RYR1-3

Gene transcript	**Comparisons between cell types**
GCG	α-cells > β-cells, α-cells > δ-cells
INS	β-cells > δ-cells > α-cells
SST	δ-cells > β-cells > α-cells
ITPR1	α-cells > δ cells > β cells
ITPR2	β-cells > δ-cells > α-cells
ITPR3	β-cells > δ-cells > α-cells
RYR1	δ-cells > α-cells, δ-cells > β-cells
RYR2	δ-cells > β-cells > α-cells
RYR3	No comparison reached statistical significance

Table 3: Number of bulk RNA-seq transcriptomes and donors across the seven accessed datasets

Study	**Profiling details**	**n**	**NG**	**HG**	**No information / between NG and HG**	**Total samples**	**Donors**
GSE116559	Purified adult β-cells	5	5	0	-	5	5
GSE57973	Purified adult β-cells	5	5	0	-	36	5
	Purified juvenile β-cells	5	5	0	-		5
	Others	26	-	-	-		3+ [a]
GSE67543	Purified fetal β-cells	6	6	0	-	24	10 [b]
	Purified adult β-cells	7	7	0	-		7
	Others	11	-	-	-		5+ [b]
GSE134068	Adult pancreatic islets		4	7	7	18	18
GSE152111	Adult pancreatic islets		17	35	14	66	66
GSE159984	Adult pancreatic islets	86	58	28	-	131	86
	Adult pancreatic islets (exposed to various conditions)	45	-	-	-		N/A[c]
Human Tissue Laboratory (HTL) dataset	Adult pancreatic islets		34	13	136	183	183
Total			**141**	**83**	**157**	***426*/463**	***385*/393**

"NG" = normoglycemic (blood glucose < 6.7 mmol/L, or non-diabetic donor), "HG" = hyperglycaemic (> 7.5 mmol/L, or type 2 diabetic donor). "No information / between NG and HG" = Blood glucose/diabetes status unknown (HTL dataset), or, blood glucose between 6.7 and 7.5 mmol/L. Sample and donor totals are shown as *total islet/β-cell preparation counts*/total preparation counts. Donors are counted only if sufficient unique metadata deposits/stated in the publication by authors. The comparison between NG and HG used 149 islet samples (79 NG, 70 HG; GSE134068, GSE152111, GSE159984); purified β-cell analyses used 17 adult, 5 juvenile, and 6 fetal β-cell samples; 21 islet samples with intermediate or

missing glucose values were used for abundance analyses only; the 45 cultured GSE159984 samples and “Others” were not analysed **(Supplementary Data 9)**.

[a]The study contained five adult and juvenile donors contributing α-/β-cells (counted once as metadata matched), eight EndoC-βH1 cell-line samples (no donor counted), and four acinar and four ductal cell donors, three of which did not match the metadata from β-cell donors (counted as 3+).

[b]The six samples were drawn from 10 pooled donors. Three fetal alpha cell samples did not match their metadata with other samples (counted as 5+).

[c]The 45 cultured islet samples originate from the donors from the study, and therefore are not counted again.

Figure 1

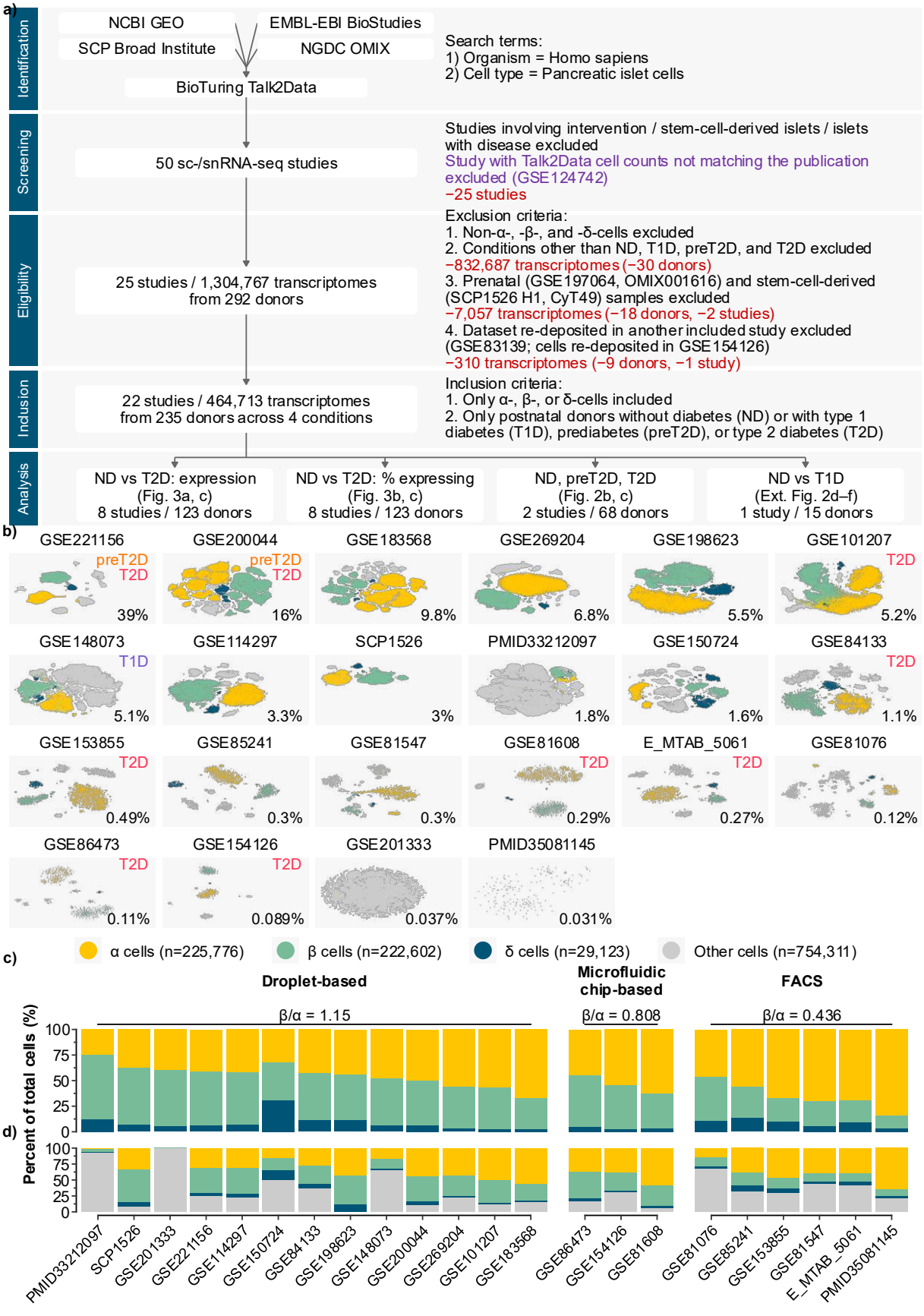
a)
Identification
NCBI GEO
EMBL-EBI BioStudies
SCP Broad Institute
NGDC OMIX
BioTuring Talk2Data
Search terms:
1) Organism = Homo sapiens
2) Cell type = Pancreatic islet cells
Screening
50 sc-/snRNA-seq studies
Studies involving intervention / stem-cell-derived islets / islets with disease excluded
Study with Talk2Data cell counts not matching the publication excluded (GSE124742)
−25 studies
Eligibility
25 studies / 1,304,767 transcriptomes from 292 donors
Exclusion criteria:
1. Non-α-, -β-, and -δ-cells excluded
2. Conditions other than ND, T1D, preT2D, and T2D excluded
−832,687 transcriptomes (−30 donors)
3. Prenatal (GSE197064, OMIX001616) and stem-cell-derived (SCP1526 H1, CyT49) samples excluded
−7,057 transcriptomes (−18 donors, −2 studies)
4. Dataset re-deposited in another included study excluded (GSE83139; cells re-deposited in GSE154126)
−310 transcriptomes (−9 donors, −1 study)
Inclusion
22 studies / 464,713 transcriptomes from 235 donors across 4 conditions
Inclusion criteria:
1. Only α-, β-, or δ-cells included
2. Only postnatal donors without diabetes (ND) or with type 1 diabetes (T1D), prediabetes (preT2D), or type 2 diabetes (T2D)
Analysis
ND vs T2D: expression (Fig. 3a, c) 8 studies / 123 donors
ND vs T2D: % expressing (Fig. 3b, c) 8 studies / 123 donors
ND, preT2D, T2D (Fig. 2b, c) 2 studies / 68 donors
ND vs T1D (Ext. Fig. 2d–f) 1 study / 15 donors
b)
GSE221156 preT2D T2D 39%
GSE200044 preT2D T2D 16%
GSE183568 9.8%
GSE269204 6.8%
GSE198623 5.5%
GSE101207 T2D 5.2%
GSE148073 T1D 5.1%
GSE114297 3.3%
SCP1526 3%
PMID33212097 1.8%
GSE150724 1.6%
GSE84133 T2D 1.1%
GSE153855 T2D 0.49%
GSE85241 0.3%
GSE81547 0.3%
GSE81608 T2D 0.29%
E_MTAB_5061 T2D 0.27%
GSE81076 0.12%
GSE86473 T2D 0.11%
GSE154126 T2D 0.089%
GSE201333 0.037%
PMID35081145 0.031%
c)
α cells (n=225,776)
β cells (n=222,602)
δ cells (n=29,123)
Other cells (n=754,311)
Droplet-based
Microfluidic chip-based
FACS
β/α = 1.15
β/α = 0.808
β/α = 0.436
d)
Percent of total cells (%)
100
75
50
25
0
PMID33212097
SCP1526
GSE201333
GSE221156
GSE114297
GSE150724
GSE84133
GSE198623
GSE148073
GSE200044
GSE269204
GSE101207
GSE183568
GSE86473
GSE154126
GSE81608
GSE81076
GSE85241
GSE153855
GSE81547
E_MTAB_5061
PMID35081145

Fig. 1: (a) A flow chart of systematic search processes from public databases is presented that demonstrates the steps involved in selecting the 22 eligible studies and 464,713 transcriptomes from 235 donors for the final analysis, and the studies and donors included in each analysis. (b) The individual plots show the tSNE projections (UMAP in the case of GSE221156 and GSE201333) of the scRNA-seq data from the 22 studies, as generated within Talk2Data **(**for display only; the embedding recorded for each study is listed in **Supplementary Data 10)**. The % value in each plot shows the percentage of the total major islet cells coming from that study. The T1D, pre-T2D, and T2D flags label the studies with cells from individuals with the condition specified in their metadata. (c) The relative percentages of major islet cells were calculated within each study and arranged in descending order of β/α-cell ratio. The studies were grouped by the cell capture techniques, across which the average β/α-cell ratio was calculated. (d) The relative percentages of the major and non-major islet cells were calculated. All non-major islet cell types were included under the 'Other' cell type.

Figure 2:

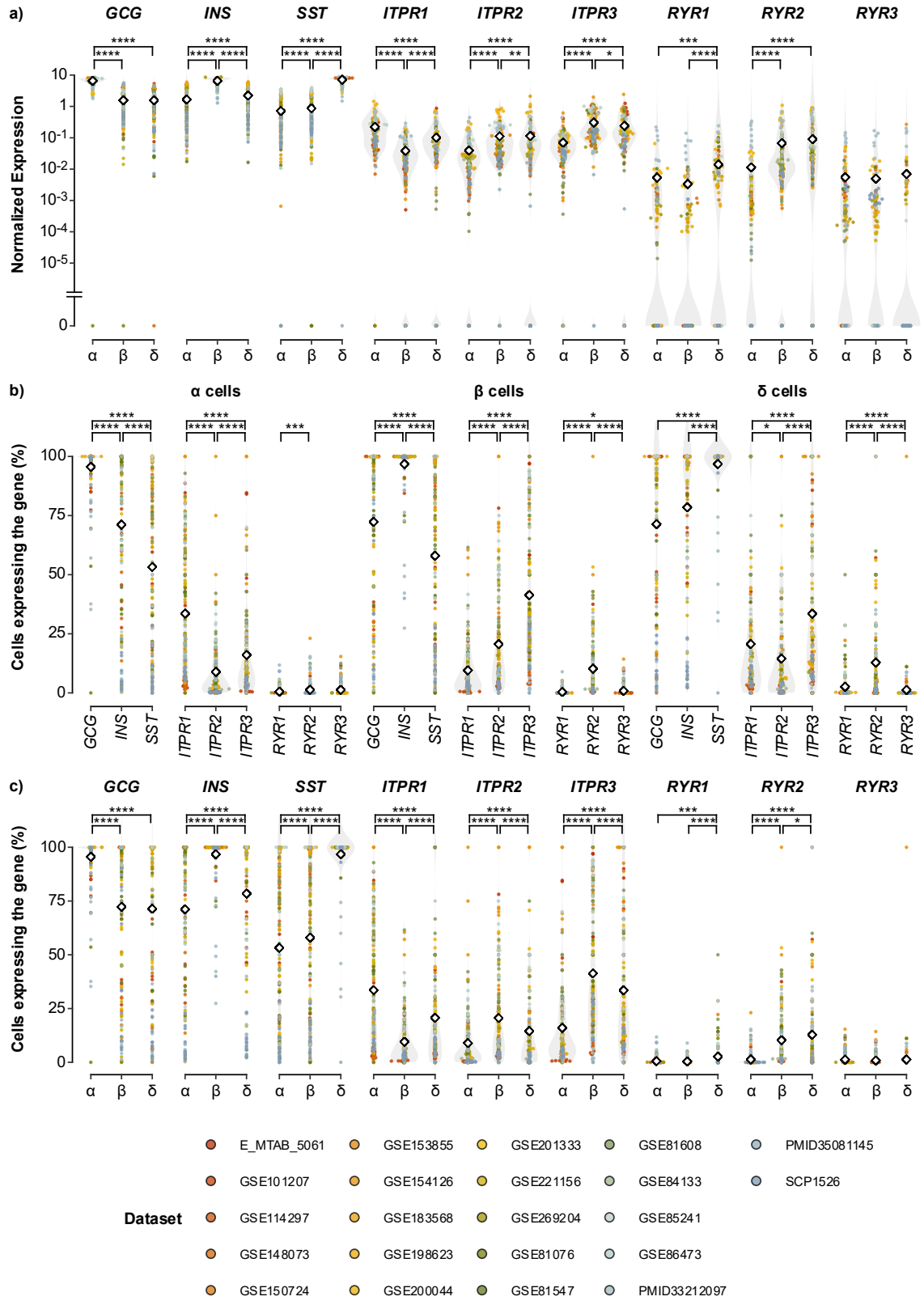
a)
GCG
INS
SST
ITPR1
ITPR2
ITPR3
RYR1
RYR2
RYR3
Normalized Expression
b)
α cells
β cells
δ cells
Cells expressing the gene (%)
c)
Dataset
E_MTAB_5061
GSE101207
GSE114297
GSE148073
GSE150724
GSE153855
GSE154126
GSE183568
GSE198623
GSE200044
GSE201333
GSE221156
GSE269204
GSE81076
GSE81547
GSE81608
GSE84133
GSE85241
GSE86473
PMID33212097
PMID35081145
SCP1526

Figure 2: (a) Level of expression (normalised reads, $\log_e$(RPM+1)) for *GCG*, *INS*, *SST, ITPR1-3* and *RYR1-3* genes in α- (n = 132,320), β- (n = 128,937), and δ- (n = 18,355) cells from individuals without diabetes were compared across the major islet cell types. Each circle represents the mean expression value at the donor level. Data were compared using Wilcoxon Signed-Rank tests (paired) within each study, and the standardised test statistics were combined (Stouffer's method) to generate an overall p-value. (b) The percentage of α-, β-, and δ-cells from individuals without diabetes expressing *ITPR1-3*, *RYR1-3, GCG, INS,* and *SST* gene transcripts was calculated for each individual. Each circle represents the percent expression value at the donor level. Data were compared using Wilcoxon Signed-Rank tests (paired) within each study, and the standardised test statistics were combined (Stouffer's method) to generate an overall p-value. (c) The percentage of α-, β-, and δ-cells from individuals without diabetes expressing *ITPR1-3*, *RYR1-3, GCG, INS,* and *SST* gene transcripts, calculated for each individual, was compared across the major islet cell types. Each circle represents the percent expression value at the donor level. Data were compared using Wilcoxon Signed-Rank tests (paired) within each study, and the standardised test statistics were combined (Stouffer's method) to generate an overall p-value. (* = p.adj < 0.05, ** = p.adj < 0.01, *** = p.adj < 0.001, and **** = p.adj < 0.0001)

Figure 3:

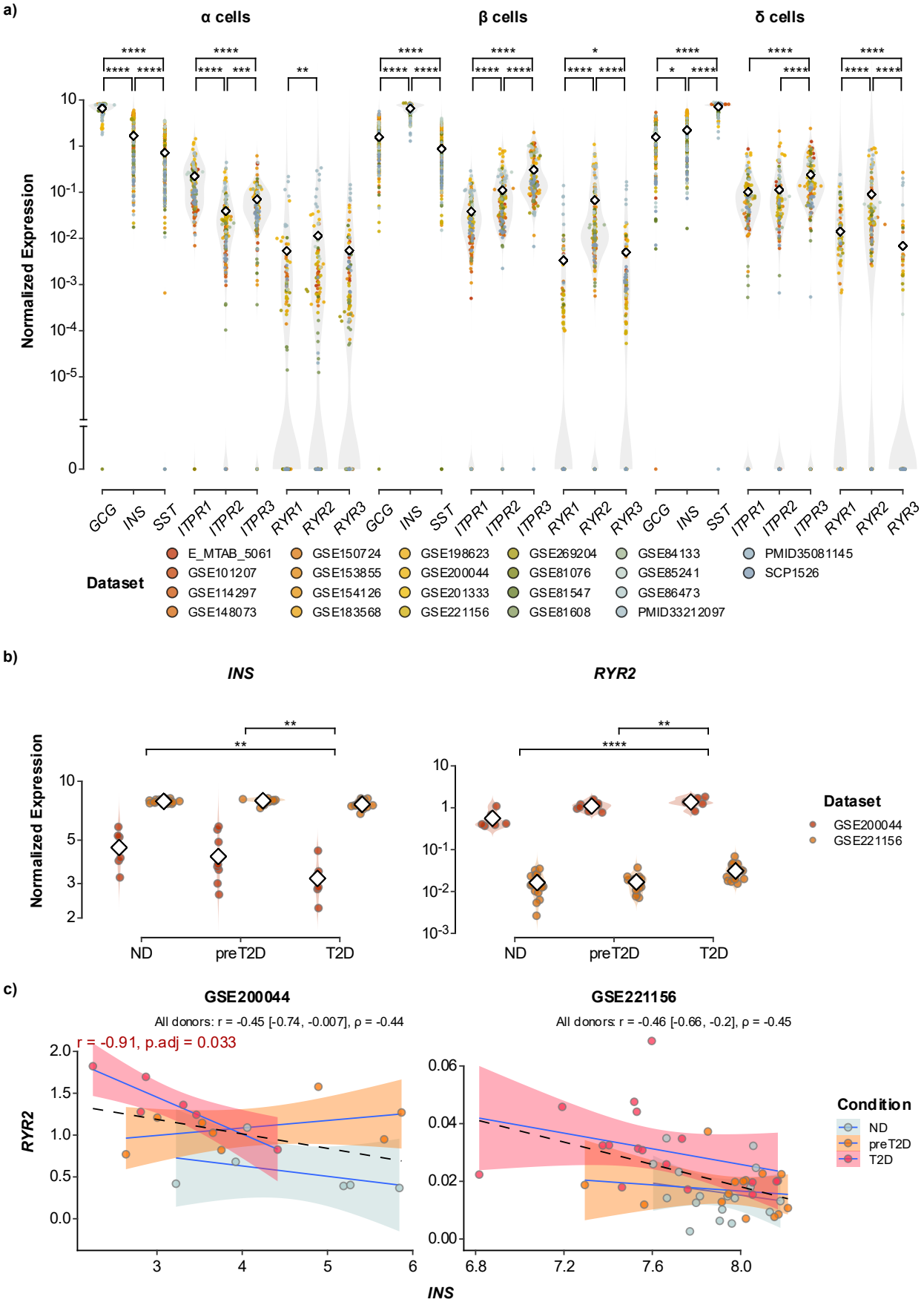
a)
α cells
β cells
δ cells
Normalized Expression
GCG
INS
SST
ITPR1
ITPR2
ITPR3
RYR1
RYR2
RYR3
Dataset
E_MTAB_5061
GSE101207
GSE114297
GSE148073
GSE150724
GSE153855
GSE154126
GSE183568
GSE198623
GSE200044
GSE201333
GSE221156
GSE269204
GSE81076
GSE81547
GSE81608
GSE84133
GSE85241
GSE86473
PMID33212097
PMID35081145
SCP1526
b)
INS
RYR2
Normalized Expression
ND
preT2D
T2D
Dataset
GSE200044
GSE221156
c)
GSE200044
GSE221156
All donors: r = -0.45 [-0.74, -0.007], ρ = -0.44
r = -0.91, p.adj = 0.033
All donors: r = -0.46 [-0.66, -0.2], ρ = -0.45
RYR2
INS
Condition
ND
preT2D
T2D

Figure 3: (a) Level of expression (normalised reads, $\log_e$(RPM+1)) for *GCG*, *INS*, *SST, ITPR1-3* and *RYR1-3* genes in α- (n = 132,320), β- (n = 128,937), and δ- (n = 18,355) cells from individuals without diabetes, extracted from the single-cell RNA transcriptome datasets. Each circle represents the mean expression value at the donor level. Data were compared using Wilcoxon Signed-Rank tests (paired) within each study, and the standardised test statistics were combined (Stouffer's method) to generate an overall p-value. (b) Donor level expression data for *INS* and *RYR2* compared across ND, preT2D, and T2D individuals for studies GSE200044 and GSE221156. (c) Pearson correlation coefficient was calculated between *INS* and *RYR2* expression for GSE200044 and GSE221156. ND, preT2D, and T2D individuals were colored separately. The dashed line shows the correlation across all donors of each study. (* = p.adj < 0.05, ** = p.adj < 0.01, *** = p.adj < 0.001, and **** = p.adj < 0.0001)

Figure 4:

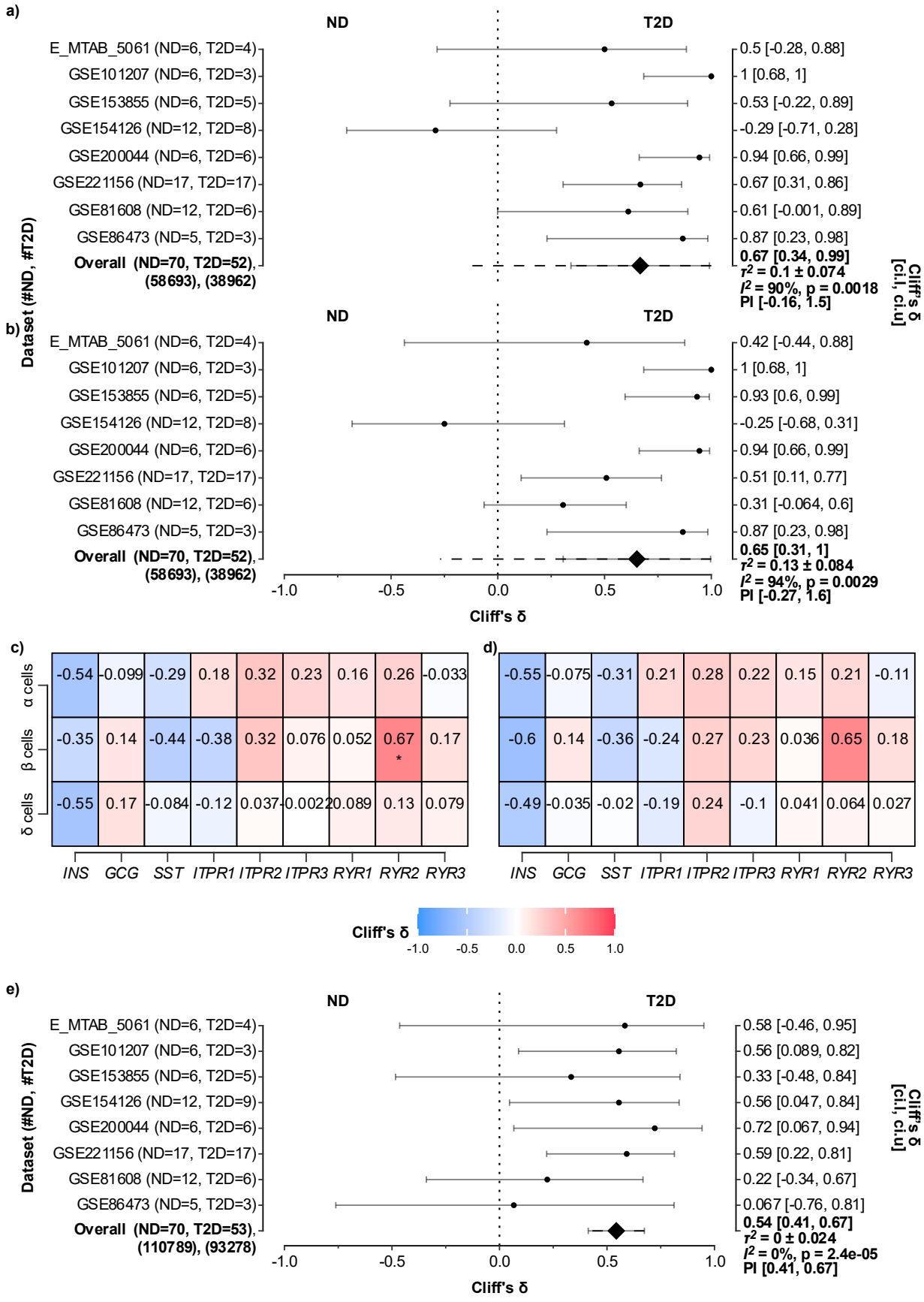
a)
ND
T2D
E_MTAB_5061 (ND=6, T2D=4)
GSE101207 (ND=6, T2D=3)
GSE153855 (ND=6, T2D=5)
GSE154126 (ND=12, T2D=8)
GSE200044 (ND=6, T2D=6)
GSE221156 (ND=17, T2D=17)
GSE81608 (ND=12, T2D=6)
GSE86473 (ND=5, T2D=3)
Overall (ND=70, T2D=52), (58693), (38962)
0.5 [-0.28, 0.88]
1 [0.68, 1]
0.53 [-0.22, 0.89]
-0.29 [-0.71, 0.28]
0.94 [0.66, 0.99]
0.67 [0.31, 0.86]
0.61 [-0.001, 0.89]
0.87 [0.23, 0.98]
0.67 [0.34, 0.99]
τ² = 0.1 ± 0.074
I² = 90%, p = 0.0018
PI [-0.16, 1.5]
Dataset (#ND, #T2D)
Cliff's δ [ci.l, ci.u]
b)
ND
T2D
E_MTAB_5061 (ND=6, T2D=4)
GSE101207 (ND=6, T2D=3)
GSE153855 (ND=6, T2D=5)
GSE154126 (ND=12, T2D=8)
GSE200044 (ND=6, T2D=6)
GSE221156 (ND=17, T2D=17)
GSE81608 (ND=12, T2D=6)
GSE86473 (ND=5, T2D=3)
Overall (ND=70, T2D=52), (58693), (38962)
0.42 [-0.44, 0.88]
1 [0.68, 1]
0.93 [0.6, 0.99]
-0.25 [-0.68, 0.31]
0.94 [0.66, 0.99]
0.51 [0.11, 0.77]
0.31 [-0.064, 0.6]
0.87 [0.23, 0.98]
0.65 [0.31, 1]
τ² = 0.13 ± 0.084
I² = 94%, p = 0.0029
PI [-0.27, 1.6]
-1.0
-0.5
0.0
0.5
1.0
Cliff's δ
c)
α cells
β cells
δ cells
-0.54 -0.099 -0.29 0.18 0.32 0.23 0.16 0.26 -0.033
-0.35 0.14 -0.44 -0.38 0.32 0.076 0.052 0.67 * 0.17
-0.55 0.17 -0.084 -0.12 0.037 -0.0022 0.089 0.13 0.079
INS GCG SST ITPR1 ITPR2 ITPR3 RYR1 RYR2 RYR3
d)
-0.55 -0.075 -0.31 0.21 0.28 0.22 0.15 0.21 -0.11
-0.6 0.14 -0.36 -0.24 0.27 0.23 0.036 0.65 0.18
-0.49 -0.035 -0.02 -0.19 0.24 -0.1 0.041 0.064 0.027
INS GCG SST ITPR1 ITPR2 ITPR3 RYR1 RYR2 RYR3
Cliff's δ
-1.0 -0.5 0.0 0.5 1.0
e)
ND
T2D
E_MTAB_5061 (ND=6, T2D=4)
GSE101207 (ND=6, T2D=3)
GSE153855 (ND=6, T2D=5)
GSE154126 (ND=12, T2D=9)
GSE200044 (ND=6, T2D=6)
GSE221156 (ND=17, T2D=17)
GSE81608 (ND=12, T2D=6)
GSE86473 (ND=5, T2D=3)
Overall (ND=70, T2D=53), (110789), (93278)
0.58 [-0.46, 0.95]
0.56 [0.089, 0.82]
0.33 [-0.48, 0.84]
0.56 [0.047, 0.84]
0.72 [0.067, 0.94]
0.59 [0.22, 0.81]
0.22 [-0.34, 0.67]
0.067 [-0.76, 0.81]
0.54 [0.41, 0.67]
τ² = 0 ± 0.024
I² = 0%, p = 2.4e-05
PI [0.41, 0.67]
Dataset (#ND, #T2D)
Cliff's δ [ci.l, ci.u]
-1.0
-0.5
0.0
0.5
1.0
Cliff's δ

Figure 4: (a) Donor-level mean RYR2 expression data were used to calculate the effect size Cliff's δ and its variance estimates, which were meta-analysed across eight studies having individuals without and with T2D. Pooled estimates are shown with Hartung–Knapp 95% confidence intervals and 95% prediction intervals (dashed lines). (b) The percentage of β-cells expressing *RYR2* was calculated at the donor level and meta-analysed across eight studies. (c) Random-effects meta-analyses compared the donor-level expression of *INS, GCG, SST, ITPR1-3,* and *RYR1-3* in the major islet cells between individuals with and without T2D across eight studies. Effect sizes (Cliff's δ) are shown with the p-values adjusted with the Bonferroni correction. (d) Random-effects meta-analyses compared the percentages of major islet cells expressing *INS, GCG, SST, ITPR1-3,* and *RYR1-3* between individuals without and with T2D across eight studies. Effect sizes (Cliff's δ) are shown with the p-values adjusted with the Bonferroni correction. (e) The proportions of pancreatic α-cells were compared across eight studies using random-effects meta-analysis. (* = p.adj < 0.05, ** = p.adj < 0.01, *** = p.adj < 0.001, and **** = p.adj < 0.0001). Donor counts for GSE154126 vary between panels a,b, and panel e, as some donors contributing β-cells and α-cells differ in this study.

Figure 5:

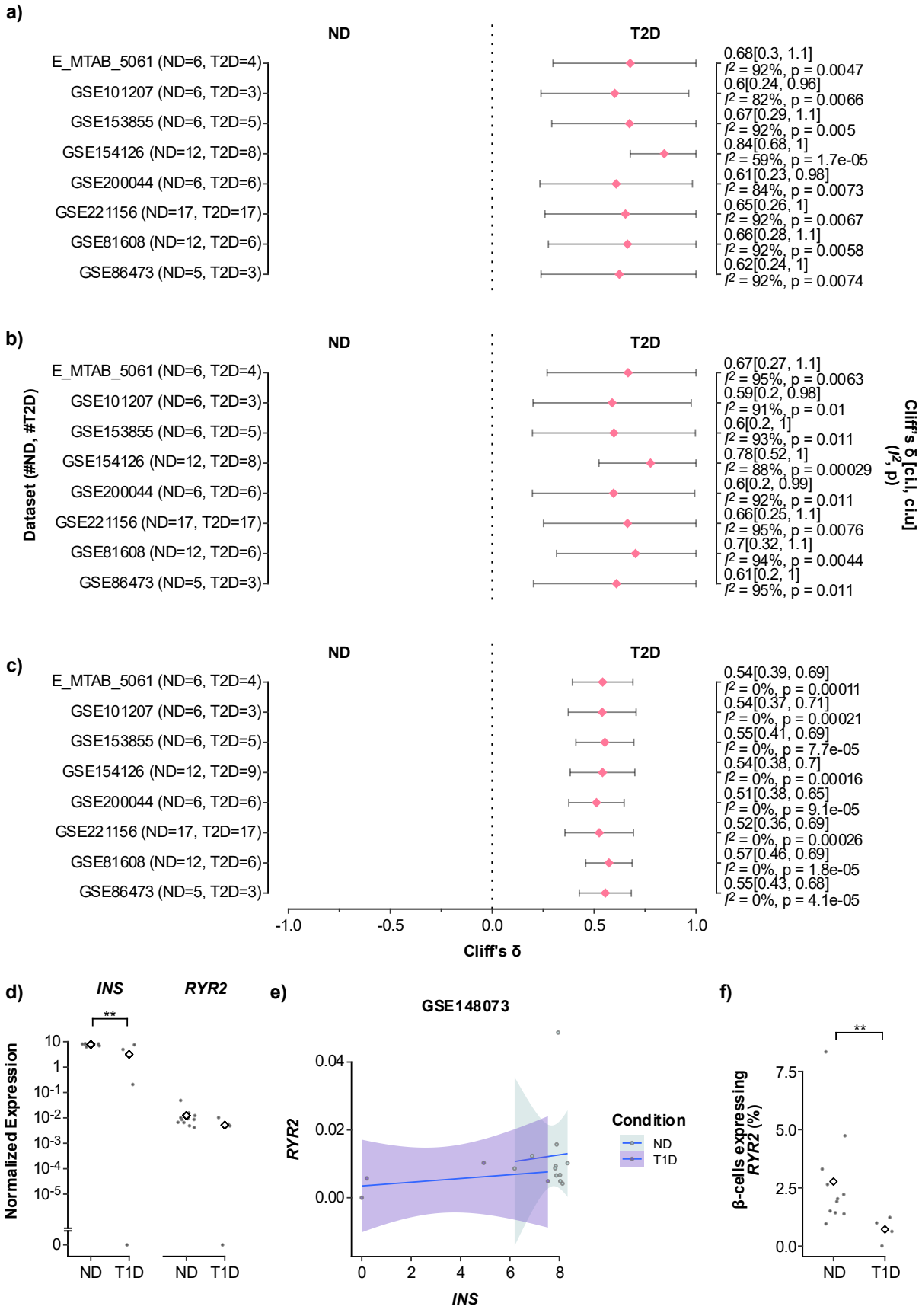
a)
ND
T2D
E_MTAB_5061 (ND=6, T2D=4)
GSE101207 (ND=6, T2D=3)
GSE153855 (ND=6, T2D=5)
GSE154126 (ND=12, T2D=8)
GSE200044 (ND=6, T2D=6)
GSE221156 (ND=17, T2D=17)
GSE81608 (ND=12, T2D=6)
GSE86473 (ND=5, T2D=3)
0.68[0.3, 1.1]
I² = 92%, p = 0.0047
0.6[0.24, 0.96]
I² = 82%, p = 0.0066
0.67[0.29, 1.1]
I² = 92%, p = 0.005
0.84[0.68, 1]
I² = 59%, p = 1.7e-05
0.61[0.23, 0.98]
I² = 84%, p = 0.0073
0.65[0.26, 1]
I² = 92%, p = 0.0067
0.66[0.28, 1.1]
I² = 92%, p = 0.0058
0.62[0.24, 1]
I² = 92%, p = 0.0074
b)
Dataset (#ND, #T2D)
Cliff's δ [c.i.l, c.i.u] (I², p)
0.67[0.27, 1.1]
I² = 95%, p = 0.0063
0.59[0.2, 0.98]
I² = 91%, p = 0.01
0.6[0.2, 1]
I² = 93%, p = 0.011
0.78[0.52, 1]
I² = 88%, p = 0.00029
0.6[0.2, 0.99]
I² = 92%, p = 0.011
0.66[0.25, 1.1]
I² = 95%, p = 0.0076
0.7[0.32, 1.1]
I² = 94%, p = 0.0044
0.61[0.2, 1]
I² = 95%, p = 0.011
c)
E_MTAB_5061 (ND=6, T2D=4)
GSE101207 (ND=6, T2D=3)
GSE153855 (ND=6, T2D=5)
GSE154126 (ND=12, T2D=9)
GSE200044 (ND=6, T2D=6)
GSE221156 (ND=17, T2D=17)
GSE81608 (ND=12, T2D=6)
GSE86473 (ND=5, T2D=3)
0.54[0.39, 0.69]
I² = 0%, p = 0.00011
0.54[0.37, 0.71]
I² = 0%, p = 0.00021
0.55[0.41, 0.69]
I² = 0%, p = 7.7e-05
0.54[0.38, 0.7]
I² = 0%, p = 0.00016
0.51[0.38, 0.65]
I² = 0%, p = 9.1e-05
0.52[0.36, 0.69]
I² = 0%, p = 0.00026
0.57[0.46, 0.69]
I² = 0%, p = 1.8e-05
0.55[0.43, 0.68]
I² = 0%, p = 4.1e-05
-1.0
-0.5
0.0
0.5
1.0
Cliff's δ
d)
INS
RYR2
**
Normalized Expression
ND
T1D
e)
GSE148073
RYR2
INS
Condition
ND
T1D
f)
**
β-cells expressing RYR2 (%)
ND
T1D

Figure 5: (a) Leave-one-out analysis for the meta-analysis of *RYR2* expression in pancreatic β cells across eight studies between individuals without and with T2D. (b) Leave-one-out analysis for the meta-analysis of the percentage of β cells expressing *RYR2* across eight studies between individuals without and with T2D. (c) Leave-one-out analysis for the meta-analysis of the number of α-cells across eight studies between individuals without and with T2D. (d) Donor-level expression of *INS* and *RYR2* was compared between individuals without and with T1D using the Wilcoxon Rank-Sum test. (e) Pearson correlation coefficient was calculated between *INS* and *RYR2* expression for GSE148073. ND and T1D individuals were colored separately. (* = p.adj < 0.05, ** = p.adj < 0.01, *** = p.adj < 0.001, and **** = p.adj < 0.0001). Donor counts for GSE154126 vary between panels a, b, and c, as some donors contributing β-cells and α-cells differ in this study.

Figure 6:

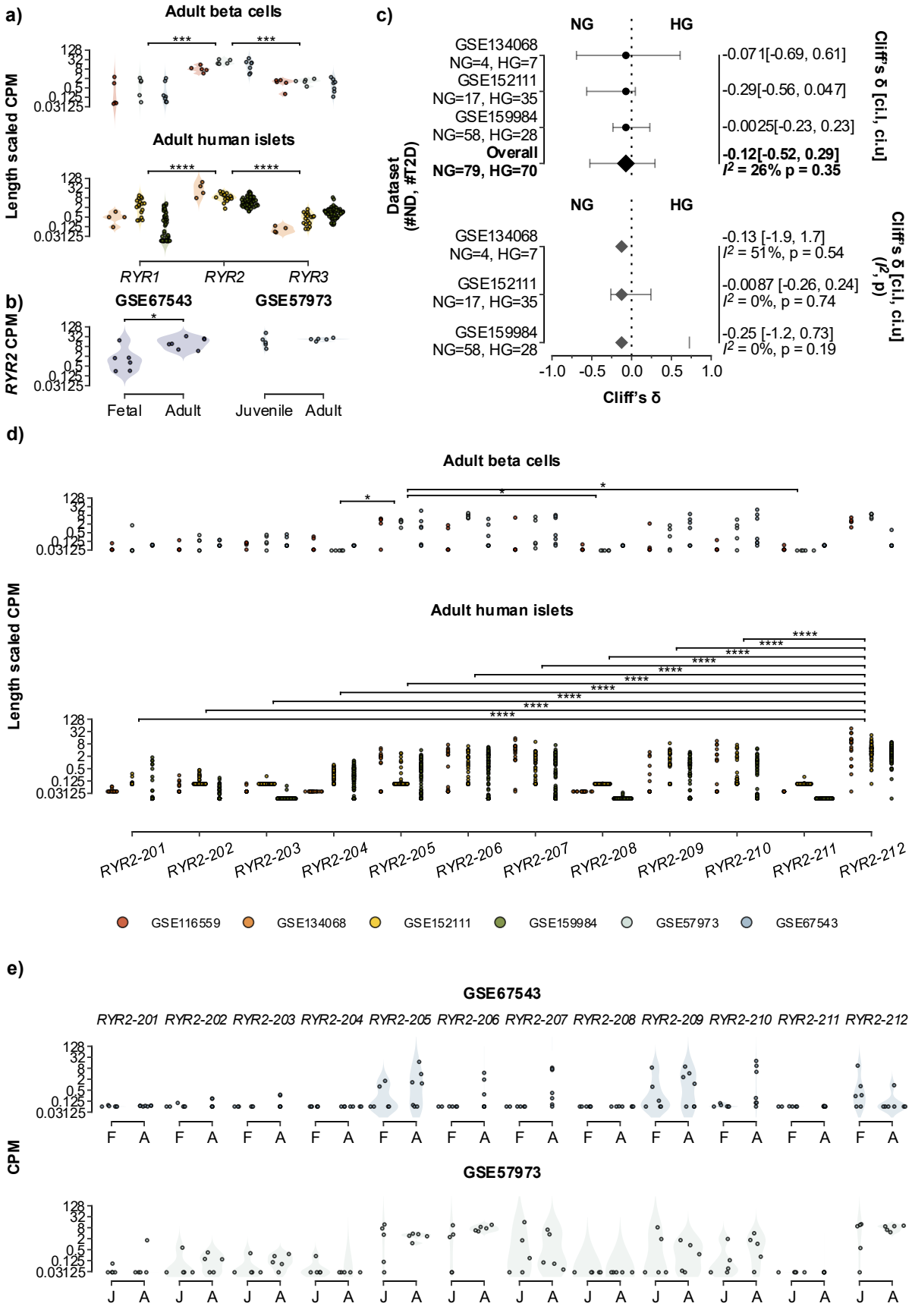
a)
Adult beta cells
Adult human islets
Length scaled CPM
RYR1
RYR2
RYR3
b)
RYR2 CPM
GSE67543
GSE57973
Fetal
Adult
Juvenile
Adult
c)
NG
HG
Dataset (#ND, #T2D)
GSE134068
NG=4, HG=7
GSE152111
NG=17, HG=35
GSE159984
NG=58, HG=28
Overall
NG=79, HG=70
-0.071[-0.69, 0.61]
-0.29[-0.56, 0.047]
-0.0025[-0.23, 0.23]
-0.12[-0.52, 0.29]
I² = 26% p = 0.35
Cliff's δ [ci.l, ci.u]
-0.13 [-1.9, 1.7]
I² = 51%, p = 0.54
-0.0087 [-0.26, 0.24]
I² = 0%, p = 0.74
-0.25 [-1.2, 0.73]
I² = 0%, p = 0.19
Cliff's δ [ci.l, ci.u] (I², p)
Cliff's δ
d)
Adult beta cells
Adult human islets
Length scaled CPM
RYR2-201
RYR2-202
RYR2-203
RYR2-204
RYR2-205
RYR2-206
RYR2-207
RYR2-208
RYR2-209
RYR2-210
RYR2-211
RYR2-212
GSE116559
GSE134068
GSE152111
GSE159984
GSE57973
GSE67543
e)
GSE67543
RYR2-201 RYR2-202 RYR2-203 RYR2-204 RYR2-205 RYR2-206 RYR2-207 RYR2-208 RYR2-209 RYR2-210 RYR2-211 RYR2-212
F A F A F A F A F A F A F A F A F A F A F A F A
CPM
GSE57973
J A J A J A J A J A J A J A J A J A J A J A J A

Figure 6 (a, d) Length-scaled transcripts per million were calculated using tximport's 'LengthScaledTPM' option, followed by edgeR's CPM calculation. CPM counts were compared within the study using the Wilcoxon Signed Rank tests (paired) followed by evidence combination. Only p-values of comparisons between RYR2-212 and other transcript variants are shown in panel d. (b) CPMs were calculated using raw counts from tximport, followed by edgeR's CPM calculation and were compared by Wilcoxon rank-sum test. (* = p.adj < 0.05, ** = p.adj < 0.01, *** = p.adj < 0.001, and **** = p.adj < 0.0001). (c) Random-effects meta-analysis and leave-one-out analysis of *RYR2* expression in NG and HG individuals. (e) Comparisons of *RYR2* transcript variants between fetal vs adult (top) and juvenile vs adult (bottom) β-cells.

Figure 7:

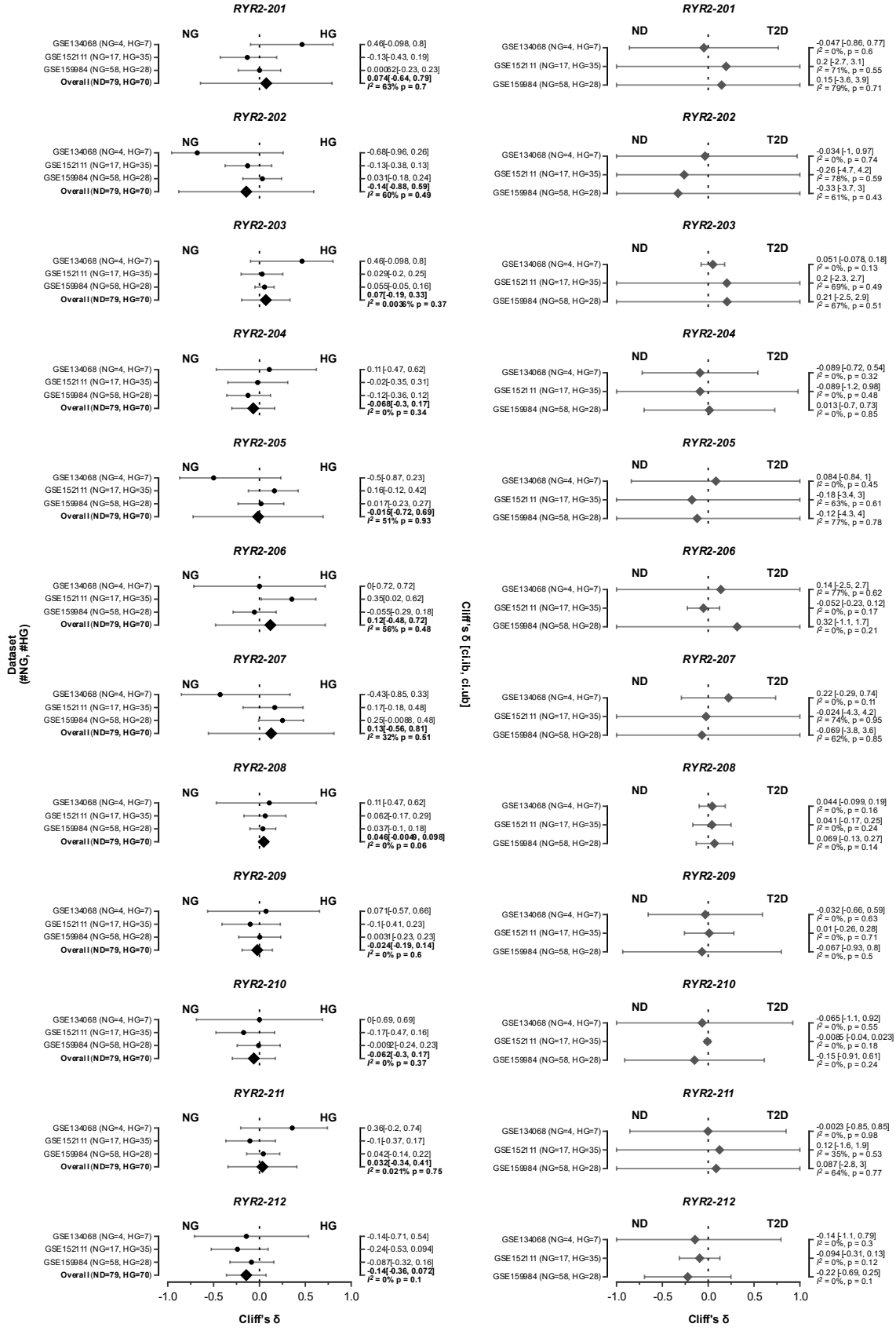
RYR2-201
NG
HG
GSE134068 (NG=4, HG=7)
GSE152111 (NG=17, HG=35)
GSE159984 (NG=58, HG=28)
Overall (ND=79, HG=70)
0.46[-0.098, 0.8]
-0.13[-0.43, 0.19]
0.00062[-0.23, 0.23]
0.074[-0.64, 0.79]
I² = 63% p = 0.7
RYR2-202
-0.68[-0.96, 0.26]
-0.13[-0.38, 0.13]
0.031[-0.18, 0.24]
-0.14[-0.88, 0.59]
I² = 60% p = 0.49
RYR2-203
0.46[-0.098, 0.8]
0.029[-0.2, 0.25]
0.055[-0.05, 0.16]
0.07[-0.19, 0.33]
I² = 0.0036% p = 0.37
RYR2-204
0.11[-0.47, 0.62]
-0.02[-0.35, 0.31]
-0.12[-0.36, 0.12]
-0.068[-0.3, 0.17]
I² = 0% p = 0.34
RYR2-205
-0.5[-0.87, 0.23]
0.16[-0.12, 0.42]
0.017[-0.23, 0.27]
-0.015[-0.72, 0.69]
I² = 51% p = 0.93
RYR2-206
0[-0.72, 0.72]
0.35[0.02, 0.62]
-0.055[-0.29, 0.18]
0.12[-0.48, 0.72]
I² = 56% p = 0.48
RYR2-207
-0.43[-0.85, 0.33]
0.17[-0.18, 0.48]
0.25[-0.0088, 0.48]
0.13[-0.56, 0.81]
I² = 32% p = 0.51
RYR2-208
0.11[-0.47, 0.62]
0.062[-0.17, 0.29]
0.037[-0.1, 0.18]
0.046[-0.0049, 0.098]
I² = 0% p = 0.06
RYR2-209
0.071[-0.57, 0.66]
-0.1[-0.41, 0.23]
0.0031[-0.23, 0.23]
-0.024[-0.19, 0.14]
I² = 0% p = 0.6
RYR2-210
0[-0.69, 0.69]
-0.17[-0.47, 0.16]
-0.0092[-0.24, 0.23]
-0.062[-0.3, 0.17]
I² = 0% p = 0.37
RYR2-211
0.36[-0.2, 0.74]
-0.1[-0.37, 0.17]
0.042[-0.14, 0.22]
0.032[-0.34, 0.41]
I² = 0.021% p = 0.75
RYR2-212
-0.14[-0.71, 0.54]
-0.24[-0.53, 0.094]
-0.087[-0.32, 0.16]
-0.14[-0.36, 0.072]
I² = 0% p = 0.1
-1.0
-0.5
0.0
0.5
1.0
Cliff's δ
Dataset (#NG, #HG)
Cliff's δ [ci.lb, ci.ub]
ND
T2D
GSE134068 (NG=4, HG=7)
GSE152111 (NG=17, HG=35)
GSE159984 (NG=58, HG=28)
-0.047 [-0.86, 0.77]
I² = 0%, p = 0.6
0.2 [-2.7, 3.1]
I² = 71%, p = 0.55
0.15 [-3.6, 3.9]
I² = 79%, p = 0.71
-0.034 [-1, 0.97]
I² = 0%, p = 0.74
-0.26 [-4.7, 4.2]
I² = 78%, p = 0.59
-0.33 [-3.7, 3]
I² = 61%, p = 0.43
0.051 [-0.078, 0.18]
I² = 0%, p = 0.13
0.2 [-2.3, 2.7]
I² = 69%, p = 0.49
0.21 [-2.5, 2.9]
I² = 67%, p = 0.51
-0.089 [-0.72, 0.54]
I² = 0%, p = 0.32
-0.089 [-1.2, 0.98]
I² = 0%, p = 0.48
0.013 [-0.7, 0.73]
I² = 0%, p = 0.85
0.084 [-0.84, 1]
I² = 0%, p = 0.45
-0.18 [-3.4, 3]
I² = 63%, p = 0.61
-0.12 [-4.3, 4]
I² = 77%, p = 0.78
0.14 [-2.5, 2.7]
I² = 77%, p = 0.62
-0.052 [-0.23, 0.12]
I² = 0%, p = 0.17
0.32 [-1.1, 1.7]
I² = 0%, p = 0.21
0.22 [-0.29, 0.74]
I² = 0%, p = 0.11
-0.024 [-4.3, 4.2]
I² = 74%, p = 0.95
-0.069 [-3.8, 3.6]
I² = 62%, p = 0.85
0.044 [-0.099, 0.19]
I² = 0%, p = 0.16
0.041 [-0.17, 0.25]
I² = 0%, p = 0.24
0.069 [-0.13, 0.27]
I² = 0%, p = 0.14
-0.032 [-0.66, 0.59]
I² = 0%, p = 0.63
0.01 [-0.26, 0.28]
I² = 0%, p = 0.71
-0.067 [-0.93, 0.8]
I² = 0%, p = 0.5
-0.065 [-1.1, 0.92]
I² = 0%, p = 0.55
-0.0085 [-0.04, 0.023]
I² = 0%, p = 0.18
-0.15 [-0.91, 0.61]
I² = 0%, p = 0.24
-0.0023 [-0.85, 0.85]
I² = 0%, p = 0.98
0.12 [-1.6, 1.9]
I² = 35%, p = 0.53
0.087 [-2.8, 3]
I² = 64%, p = 0.77
-0.14 [-1.1, 0.79]
I² = 0%, p = 0.3
-0.094 [-0.31, 0.13]
I² = 0%, p = 0.12
-0.22 [-0.69, 0.25]
I² = 0%, p = 0.1
Cliff's δ [ci.l, ci.u] (I²,p)

Figure 7: Random-effects meta-analyses compared the expression of twelve transcript variants of *RYR2* between individuals without and with T2D across three studies.

Supplementary Figure 1:

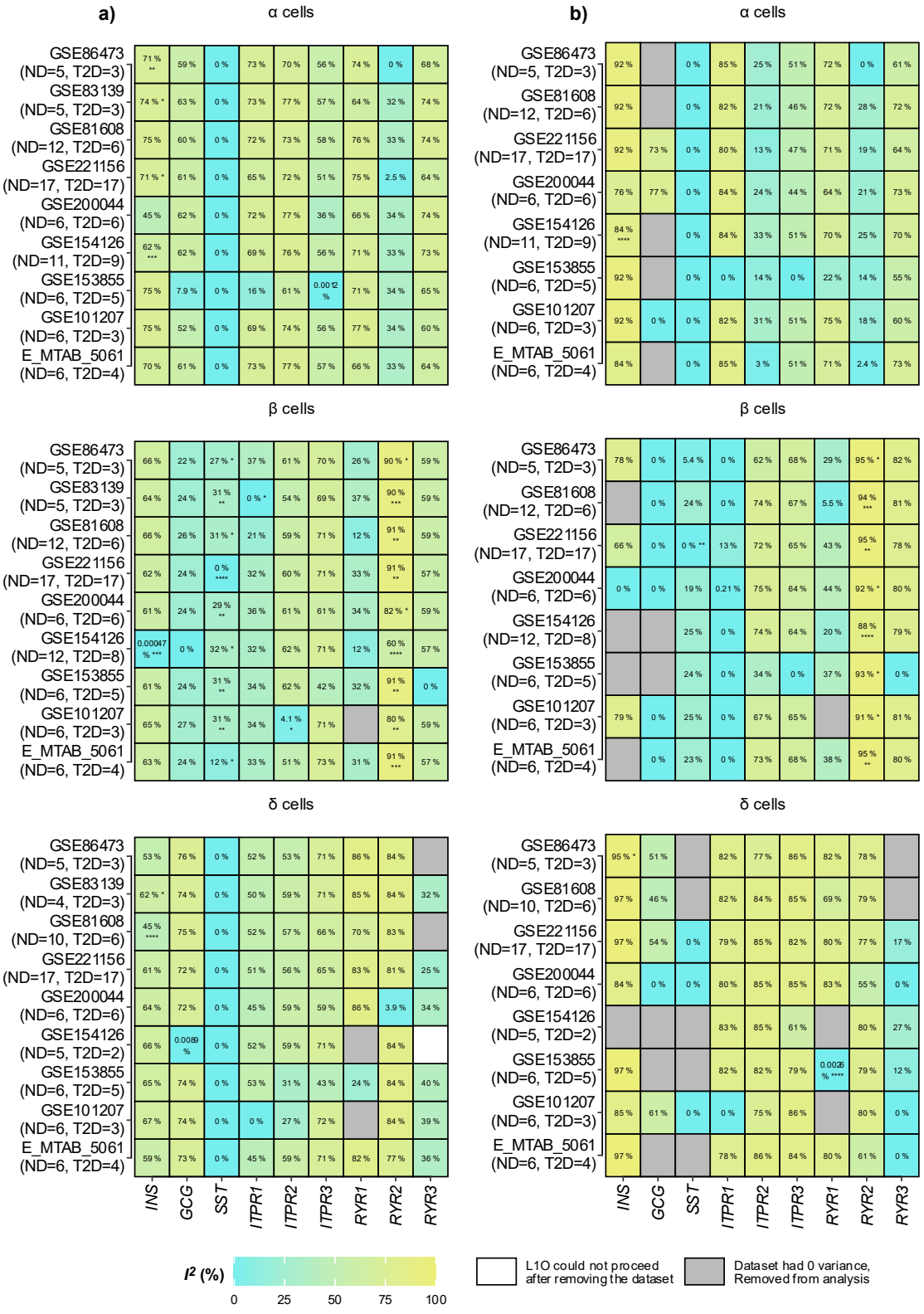

Supp. Fig. 1: Leave-one-out analyses for the meta-analyses comparing the (a) expression and (b) percentage expression of nine transcripts across three major islet cell types across studies. (* = p.adj < 0.05, ** = p.adj < 0.01, *** = p.adj < 0.001, and **** = p.adj < 0.0001).

Supplementary Figure 2:

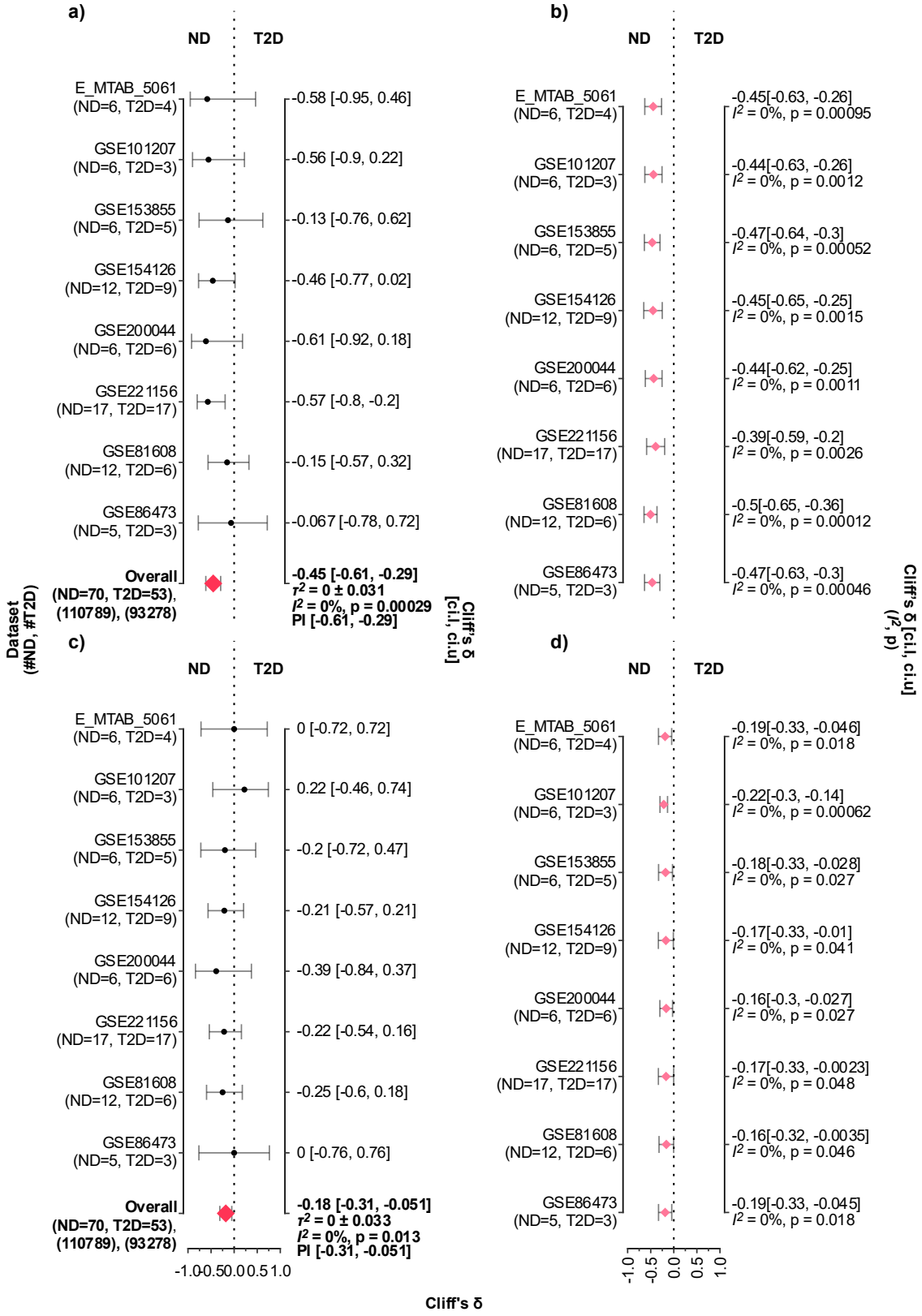

Supp. Fig. 2: (a, c) Random-effects meta-analysis of the proportions of β- and δ-cells (relative to all α-, β-, and δ-cells captured per donor) across eight studies between individuals without and with T2D and (b, d) corresponding leave-one-out analyses.

Supplementary Figure 3:

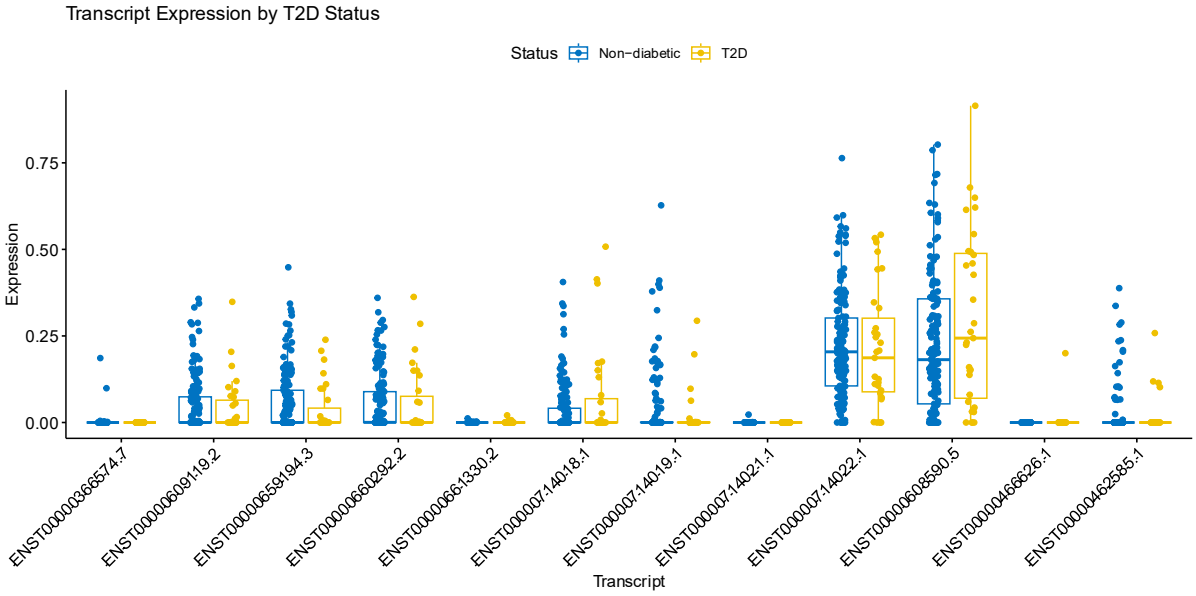

Supp. Fig. 3: log_2-transformed TPM abundances of *RYR2* transcript isoforms were compared between non-diabetic (ND) and T2D individuals in the HTL dataset using a limma framework modelling transcript expression as a function of T2D status, controlling for age, gender, BMI, purity, and days cultured.

Supplementary Figure 4:

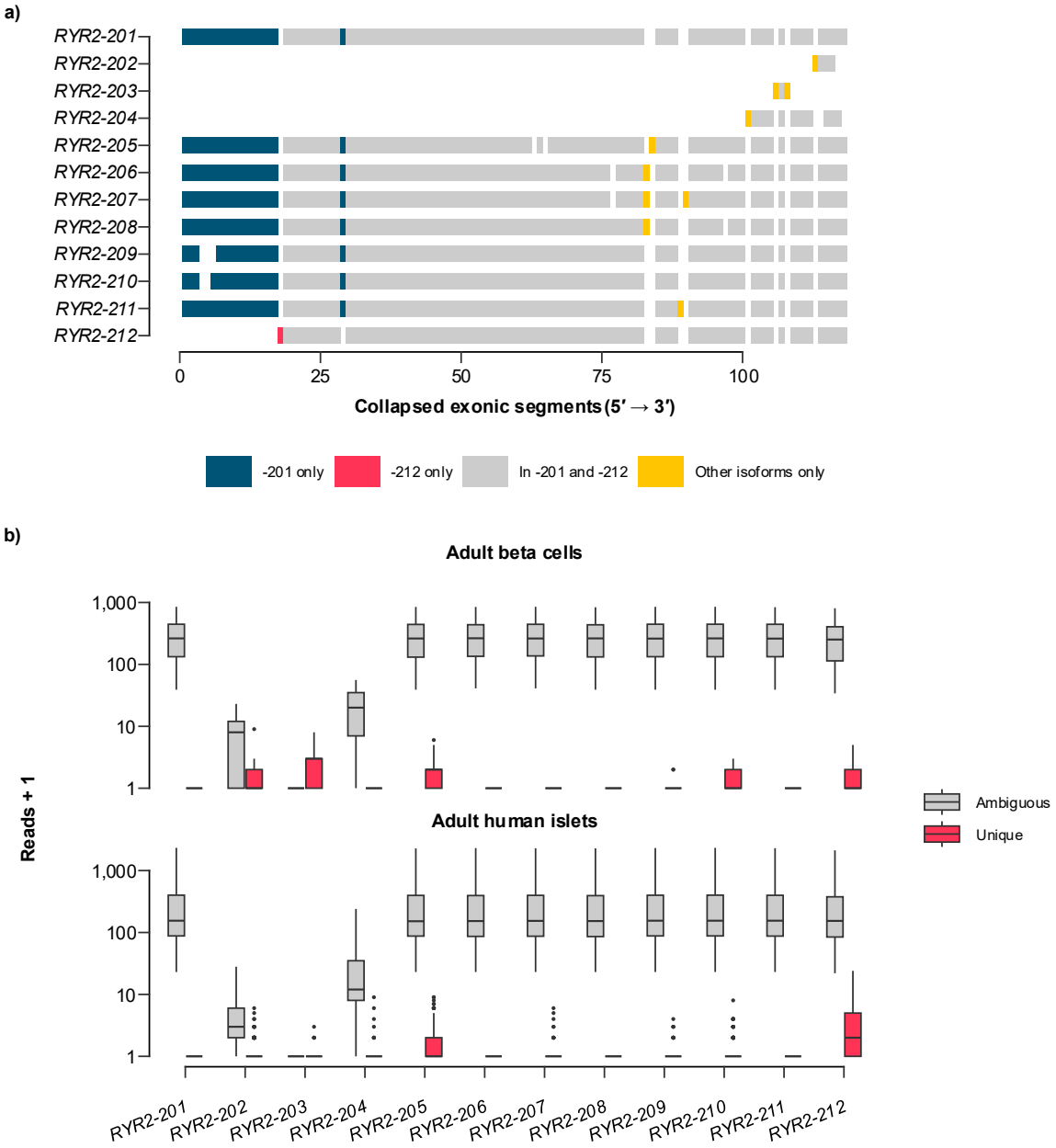

Supp. Fig. 4: (a) Exonic structure of the twelve *RYR2* transcript variants (GENCODE release 48), shown as collapsed exonic segments (5′ to 3′) and coloured by whether each segment is present only in *RYR2-201*, only in *RYR2-212*, in both, or only in other variants. (b) Reads assigned by Salmon to each *RYR2* transcript variant that are unique to that variant or ambiguous (compatible with more than one variant), per sample, in adult purified β-cells (n = 17) and adult human islets (n = 215), shown as reads + 1 on a log scale.

Supplementary Figure 5:

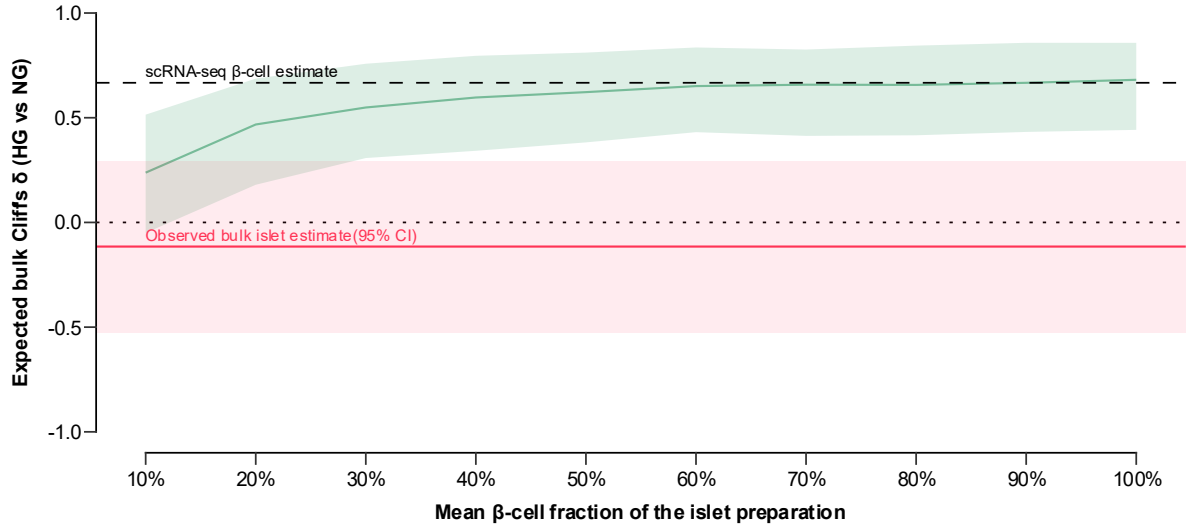

Supp. Fig. 5: Expected bulk-islet Cliff's δ (HG vs NG) for *RYR2* if the increase seen in scRNA-seq β-cells (Cliff's δ = 0.67, dashed line) were restricted to β-cells and diluted by non-β-cell transcripts, simulated across mean β-cell fractions of the islet preparation (green line, median; band, 95% interval of 500 simulations with 30 donors per group). Between-donor variability (s.d. 1.2 on the log scale) and the ratio of non-β-cell to β-cell *RYR2* expression (0.29) were estimated from the scRNA-seq data of donors without diabetes. The observed bulk islet estimate (Cliff's δ = −0.12) and its 95% CI are shown in red.

Supplementary Figure 6:

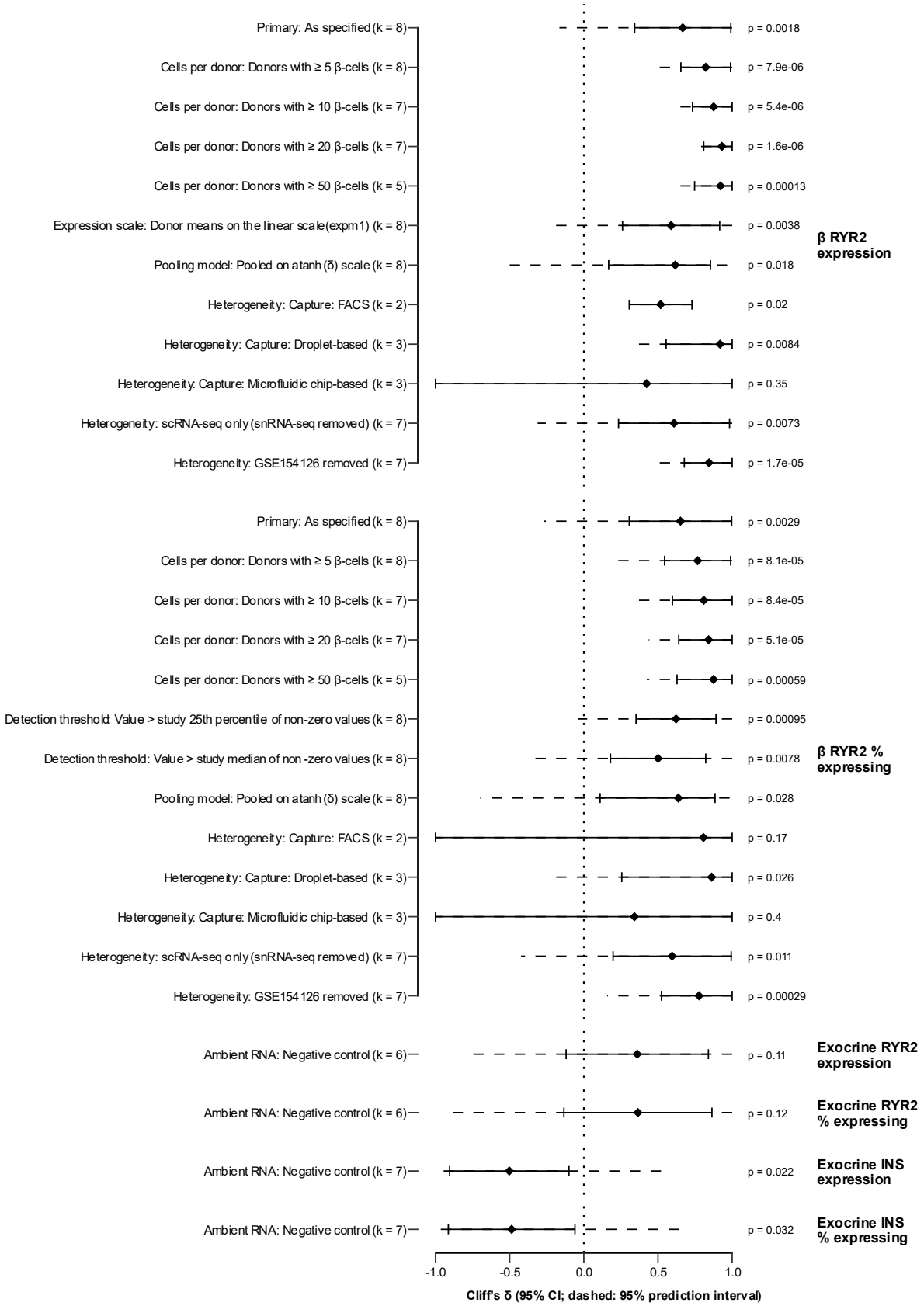

Supp. Fig. 6: Sensitivity analyses of the random-effects meta-analyses comparing β-cell *RYR2* expression and the percentage of β-cells expressing *RYR2* between individuals without and

with T2D: restriction to donors with at least 5, 10, 20, or 50 β-cells, donor means on the linear scale, stricter detection thresholds (above each study's 25th percentile or median of non-zero values), pooling on the atanh(δ) scale, subgroups by cell-capture method, exclusion of snRNA-seq data, and exclusion of GSE154126. Exocrine cells were analysed as a negative control for ambient RNA. Diamonds show pooled Cliff's δ with 95% confidence intervals (solid) and 95% prediction intervals (dashed); k, number of studies; P values are not adjusted for multiple comparisons. Values are listed in **Supplementary Data 1**.

Supplementary Files

This is a list of supplementary files associated with this preprint. Click to download.

- suppFig2.svg
- suppFig3.svg
- SupplementaryData.xlsx
- suppFig1.svg
- suppFig5.svg
- suppFig6.svg
- suppFig4.svg